



**HAL**  
open science

## On-site pXRF analysis of body, glaze and colouring agents of the tiles at the excavation site of Iznik kilns

Gulsu Simsek, Belgin Demirsar Arli, Sennur Kaya, Philippe Colomban

### ► To cite this version:

Gulsu Simsek, Belgin Demirsar Arli, Sennur Kaya, Philippe Colomban. On-site pXRF analysis of body, glaze and colouring agents of the tiles at the excavation site of Iznik kilns. *Journal of the European Ceramic Society*, 2019, 39 (6), pp.2199-2209. 10.1016/j.jeurceramsoc.2019.01.050 . hal-03940426

**HAL Id: hal-03940426**

**<https://hal.science/hal-03940426>**

Submitted on 16 Jan 2023

**HAL** is a multi-disciplinary open access archive for the deposit and dissemination of scientific research documents, whether they are published or not. The documents may come from teaching and research institutions in France or abroad, or from public or private research centers.

L'archive ouverte pluridisciplinaire **HAL**, est destinée au dépôt et à la diffusion de documents scientifiques de niveau recherche, publiés ou non, émanant des établissements d'enseignement et de recherche français ou étrangers, des laboratoires publics ou privés.

**On-site pXRF analysis of glaze, body composition and colouring agents of tiles of kilns excavation at Iznik**

Gulsu Simsek<sup>1</sup>, Belgin Demirsar Arli<sup>2</sup>, Sennur Kaya<sup>3</sup>, Philippe Colomban<sup>4</sup>

<sup>1</sup> Koç University Surface Science and Technology Center (KUYTAM), Rumelifeneri Yolu, Sariyer 34450 Istanbul, Turkey

<sup>2</sup> Istanbul University, Faculty of Letters, Department of Art History, Balabanaga Mah., Laleli, Fatih, Istanbul

<sup>3</sup> Istanbul University, Department of Fine Arts, Balabanaga Mah. Laleli, Fatih, Istanbul

<sup>4</sup> Sorbonne Université, CNRS, MONARIS, Campus Pierre-et-Marie Curie, 75005, Paris, France

*corresponding author:* [qusimsek@ku.edu.tr](mailto:qusimsek@ku.edu.tr)

Tel +902123381768; fax +902123381559

# On-site pXRF analysis of glaze, body composition and colouring agents of tiles of kilns excavation at Iznik

Gulsu Simsek<sup>1</sup>, Belgin Demirsar Arli<sup>2</sup>, Sennur Kaya<sup>3</sup>, Philippe Colomban<sup>4</sup>

<sup>1</sup> Koç University Surface Science and Technology Center (KUYTAM), Rumelifeneri Yolu, Sariyer 34450 Istanbul, Turkey

corresponding author: [gusimsek@ku.edu.tr](mailto:gusimsek@ku.edu.tr)

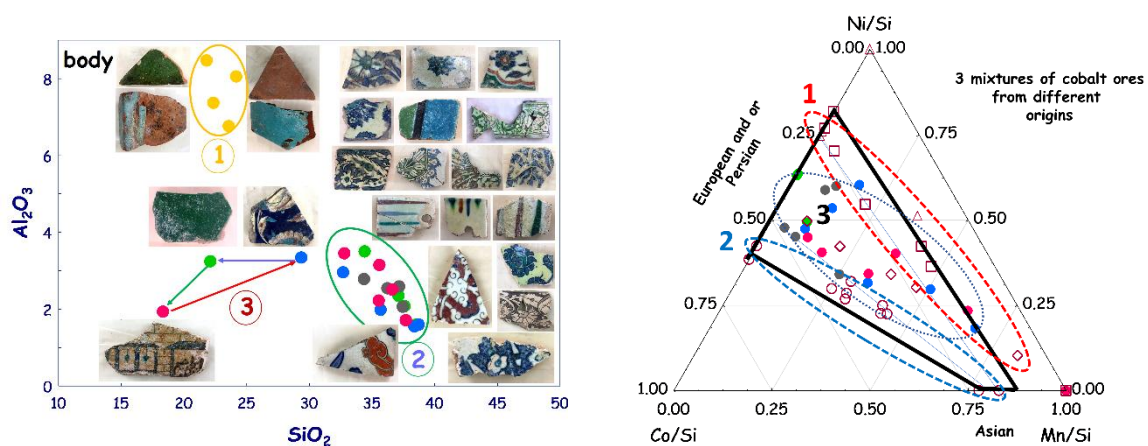
<sup>2</sup> Istanbul University, Faculty of Letters, Department of Art History, Balabanaga Mah., Laleli, Fatih, Istanbul

<sup>3</sup> Istanbul University, Department of Fine Arts, Balabanaga Mah. Laleli, Fatih, Istanbul

<sup>4</sup> Sorbonne Université, CNRS, MONARIS, Campus Pierre-et-Marie Curie, 75005, Paris, France

## Abstract

The excavations in Iznik, which aim to present the history and cultural heritage of the city, had started in 1969 in the sites of Orhan İmaret and its Bath (Turkish Hamam) and continued for kilns. We present here the first on-site, non-invasive analyses performed with portable XRF (pXRF) instrument in twenty-five excavated tiles both glazed and unglazed, and two residue materials of the kiln. The shards studied were attributed to the productions from 14th- to 17th-centuries. Comparison is made between the discussion of characteristic elemental composition ratio selected from ceramic technology criteria and PCA/Euclidian diagram analyse. Three groups of body composition were evidenced: 1- rich in clay, poor in quartz and 2- poor in clay, rich in quartz as previously demonstrated and linked to Timurids heritage and characteristic of Iznik potter innovation, respectively; and 3- a new group, a mixture of quartz, clay, and chalk. We encountered three different glazing technologies: Sn-rich, Sn-medium and Sn-poor glazes. The amount of tin oxide in the glaze decreases by centuries. Besides, two different types of fluxes used in the glaze, some containing only potassium, and the others having potassium and calcium. The decors, which were investigated in this study were blue, turquoise, green, red colours, and black lines. Three mixtures of cobalt ores were determined. The blue pigments from European cobalt sources are a mixture of Co-Ni-Fe-As. The Chinese-like source was also determined in some of the tiles without arsenic and the ratio of Mn versus Co > 1. The third cobalt source contains Mn/Co < 1 without arsenic. Most of the red colours contains iron but some with a mixture of copper and iron consistent with the use of the bornite ( $\text{Cu}_5\text{FeS}_4$ ) mineral from Anatolian (Turkey) mining, not documented before in Iznik decors. Spinel or chromite-based pigments were used in the drawings of black lines. Green areas contain copper or chrome containing pigments. The addition of copper lead to turquoise colour.



ajouter figure sur glaze ou cobalt

**Keywords:** A: Excavation; B: Iznik; C: Portable XRF instrument (pXRF); D: Ottoman ceramics; E: Kilns; F: Tiles

## 1. Introduction

The excavations in Iznik, which aim to present the history and cultural heritage of the city, had started in 1969 in the sites of Orhan Imaret and its Bath (Turkish Hamam) and continued for kilns. [1] Iznik, which was being called as Nicaea under the Byzantium rule, placed at the intersection of the roads linking the Middle-East region to the Balkan states through Anatolia since 4th-century BC. [2] Iznik came into prominence when the ceramic production had developed during the Ottoman Empire. The excavation work of Iznik tiles kilns continues as the third period of the field mission [3]. The origin of Iznik technology remains debated because the links with the know-how of Seljuk, Timurid, and Byzantine productions of Nicaea are not well defined due to the limited studies carried out at the excavation site and on the ancient Ottoman buildings historically well documented. Most of the architecture, holy places, mosques, and similar, built in Istanbul, Edirne, and Bursa have with the "Iznik" style tiles ornamented [4-10]. Indeed, the Ottoman sources state that the Iznik production was used more as a trade name than a provenance [11]. This study aims to identify the technology of tiles produced in the kilns of Iznik city and define the technological links between Timurid and Seljuk productions.

Since the 1980s, mostly laboratory studies with large-scale, destructive instruments and few on-site measurements with some portable, non-destructive techniques were conducted about the characterization of Ottoman period ceramics, where the research on Iznik and Kütahya productions lead, by international [12-20] and national researchers [21-25]. Mainly, the material studied on-site concerns of the collections of the museums [19,20], and rarely on buildings [25]. The place or places of production of "Iznik" style ceramics are still debated, the number of shards found in the excavation context is reduced and the measurements have been focused more on the analysis of paste and mostly published in an inaccessible form for the international researchers due to the national language used [1,11,27,28]. The analyses concerning the colouring agents are old and limited to a few fragments whose origin is poorly or not documented. The most comprehensive work comprises the analyses of the shards preserved in the vaults of Topkapi Palace Museum with scanning electron microscopy-energy dispersive spectrometer (SEM-EDS) and Raman instruments [11,26,27]. The aim was to characterize non-inventoried shards and attribute the productions of Iznik, Kütahya, Tekfur Palace (Istanbul), and some other Ottoman ceramics of unknown origin by comparing the microstructure of the cross sections, glaze signatures and chemical composition of the bodies, glazes, and pigments found in the decors. The reference materials were selected among the tiles of known origin, which was already recorded in the inventory of the museum or buildings, where they were used.

On the contrary to the analyses of movable and immovable cultural assets of Iznik production, very few works were conducted on the excavation materials of Iznik tile kilns and the studies were performed only with the destructive techniques [2,28-30]. During her Ph.D. work, Füsün Okyar [28] performed petrographic and chemical analyses of the bodies, slips, glazes, and coloured decors of the shards of redware and stone-paste type, in total twenty-four samples. Chemical compositions were defined with SEM-EDS method. The research on the excavation materials continued with the studies of T. Tulun and her colleagues by using similar techniques to identify the technological properties [2]. The advantage of the use of laboratory-type instruments is the possibility of a multi-scale analysis of the sections (including glaze, decor, slip, and body) of the shards. The high-resolution techniques, including petrographic microscopy, SEM-EDS, micro-XRD (X-rays diffraction), micro-XRF (X-rays fluorescence), and micro-Raman, with high detection capabilities, are the best approaches to understand the differences and common points in the ceramic production technologies. Due to the destructive character of the techniques, ethical rules of cultural heritage studies now limit these types of analyses as much as possible. Moreover, the shards from Iznik kilns are rare and the research ethic, especially in Turkey, covers the use of non-destructive techniques to maintain the integrity of the samples. Due to the complexity of the Iznik decors with superposition of several layers of enamels, the analysis by micro-techniques imposes one of the cuts incompatibles with the respect of the artifacts. In addition, most of the documented "Iznik" tiles are in UNESCO World Heritage sites and their analysis can be only non-invasive. Therefore, the portable, non-destructive techniques, e.g., pXRF, pRaman, and FORS (Fiber Optics Reflectance (UV-nIR) Spectroscopy) have become essential tools for the analyses of the objects in place (tiles) or exclusive objects preserved in the secure rooms of museums or private collections. Thus, a methodology must be created to make the analytical procedures more reliable when using portable instruments.

Moreover, the main drawback of studying the excavation materials is the interpretation of the results regarding the production technology. Because the materials, which were found at the excavation site, may be trials of the artist to define the best recipe for the artwork he/she prepare and some rejected ceramics due to the inappropriate temperature and atmosphere control of the kiln or wrong choice of the raw materials for the body and glaze. However, the tile shards found in the kiln are in general statistical representatives of the production and can be compared with the tiles found in the wall revetments of the buildings. The portable instruments, which allow non-invasive and fast measurements, help to analyse a huge number of artefacts leading a statistical approach which compares the tiles of the excavation sites with the tiles mounted on the walls of the buildings of similar periods. But, a few numbers of tiles can be extracted to be cut and prepared for the destructive methods at the laboratory which will provide individual data rather than a cumulative knowledge. Therefore, the portable, non-destructive techniques gain

importance from day to day. Thus, defining the provenance of the collections will be supported by investigating the excavation materials.

This study presents the characterization of twenty-five shards excavated recently and two residue materials formed on the walls in the Iznik tile kilns. The work has two objectives: i) the comparison of elemental data analyse based on the comparison of elemental ratio characteristic of the ceramic technology with the 'blind' approach using PCA and Euclidian dendrograms; ii) a better knowledge of the production of Iznik kilns; the results of pXRF measurements will correlate the previous measurements carried out on the excavation materials with large-scale laboratory-type instruments in order to assess the capabilities of the portable XRF system.

## **2. Experimental**

### 2.1. Tile shards

Twenty-three glazed shards and two shards not glazed but one painted and the other non-painted, were examined with the pXRF instrument in this study in addition to the measurement of kilns residues on-site and in the excavation lab. Fig. 1 shows all the studied shards which were excavated from the Iznik tile kilns. The shards shown on the first three lines were attributed to the production of 14th-16th centuries and shards on the last line are assumed to be later productions of the 17th-century. In addition to the ceramic fragments, one fall-out material (see Fig. S1), which were formed on the walls inside the kiln, was measured with pXRF. The detailed information about the tiles studied is given in Table S1. The dating of the shards was determined aesthetically by the director and sub-director of Iznik tiles kilns excavations related to the building, where similar types of tiles were used [32-34]. On the contrary to tableware production, tiles were always produced by order of the Sultans to be used as wall decorations, in the architectural buildings, holy places, mosques, etc. Therefore, the production date of the tiles is much better documented compared with the tableware ceramics. Furthermore, the aesthetical and technical characteristics of the tiles change through the centuries. Ottoman ceramic art technology started with both coloured glaze and underglaze decor but with changing the quality of the body and glaze composition, and colours in the decors. With the regression of the refined structure of Iznik ceramics from 17th-century, poorer quality of paste and glaze [9,10,17,19,35], decorated with coarse patterns seem on the tiles which were produced for e.g., Blue Mosque, Valide Sultan Mosque (Eminönü, Istanbul). Additionally, the dating of the tiles was determined depending on the restoration records of the buildings [1,34].

Out of the intact tiles, one fall-out material (F1) of the unattributed period (15th-, 16th- or 17th-c.), which was formed on the walls of the kiln, is measured with pXRF. Besides, one measurement at the kiln site was performed on the walls of the kiln in order to identify the chemical composition of the green formation (see Fig. S2).

Among the tiles of 14th and 16th-centuries (Fig. 1), four of them (B8-0, B7-1, A7-3, B8-1) have monochrome glazes and red bodies rather similar to hexagonal tiles of Yesil Camii (Bursa, 1424-1429), Muradiye Camii (Bursa, 1426), Muradiye Camii (Edirne, 1435-1436) and Şah Melek Paşa, Camii (Edirne, 1429). These shards are thicker than the others, like a brick. Additionally, another shard in triangle form (A7-4) which is assumed to be included in the same group is fired but not painted and glazed (biscuit form). Three tiles (B7-11, B7-12, B7-13) of the group seem as being prototypes, where the artisan may try to determine different tonalities of the primary colours (blue, red, and green). Six shards (B7-8, B7-10, B7-15, B7-16, A7-1, A7-2) belong to the group of the classical, polychrome "Iznik" tiles as observed in . The last five tiles (B7-4, B7-5, B7-6, B7-17, and B7-3) of this group are painted in triple colours (blue-white-turquoise), just one being unglazed but already decorated. B7-3 is an example representing the technology of underglaze painting.

The 17th-century tiles include two shards (B8-2, B7-9) with under-glaze decoration in three colours (blue-white-turquoise) as observed. The other shard (B7-2) has also been decorated in triple coloured glaze being turquoise, green and dark blue thick contour. Three of them (B7-14, B8-3, and B7-7) are polychromic, one decorated with the pattern of Kaaba. F1 is a fall-out material, which was formed on the wall of the kiln as a brown glaze layer. In the case of lead-rich glazes, when the firing temperature is above 850 °C, lead oxide (PbO) vapour starts to deposit on the walls of the kiln since it is quite volatile.

## 2.2. Technique

Elemental, semi-quantitative measurements were carried out non-destructively with a hand-held X-Ray Fluorescence spectrometer positioning the Hitachi X-MET 8000 Expert Geo (Oxford Instruments) in contact with the tiles. The instrument was equipped with a rhodium (Rh) target X-ray tube of 4W, 50kV max and a silicon drift detector (SDD). It has operated by using the Mining LE method, in which two shots were performed, one at the lower energy (10 keV) for determining low Z elements (Mg and higher Z number) essentially for the body composition, and the second at the high energy (40 keV) to identify the network modifiers, colouring agents found inside the glaze. The beam size at the surface is 10.7mm x 9.4 mm, and a camera is used for controlling the measured area. Due to the variation of the minerals found in the body and the glaze thickness, the measurements were carried out on at least three different areas of the paste and coloured areas of the glaze, with 30s of radiation time (one day campaign of measurements in the excavation laboratory and excavation site by G. Simsek). The results, which are obtained as the mean values of all the individual point analyses were done on the body and each colour of the decor including the transparent glaze layer, are reported concerning weight percent (see Table S2). They were calculated via the method already installed in the instrument. For the semi-quantitative evaluation purposes, the  $K_{\alpha}$  lines of major elements Mg, Al, Si, K, Ca, transition metal elements (Ti, V, Cr, Mn, Fe, Co, Ni, Cu, Zn, As) and trace elements (Rb, Sr, Zr, Ba, Bi), as well as the L spectral lines of lead and tin, were taken into consideration. The calibration of the instrument was controlled by using the mineral standards, which allow measuring ceramic materials with a

high detection capability. For some easier comparison with the literature, some data were also transformed in wt % oxide. A pXRF system cannot measure sodium (Na) and lighter elements because of the air absorption, contrary to WD-XRF (wavelength dispersive – X-ray fluorescence) laboratory instruments, which can measure the elements up to boron in the periodic table [36]. A vacuum pump is required during the measurement of light elements, but it is not adapted for each pXRF instrument and for most in situ recording conditions regarding large tile walls. However, the amount remained after the subtraction of the sum of the other oxides from 100 refers to an approximate content of Na<sub>2</sub>O. This calculation is mainly applicable for the ancient ceramics because the major and minor constituents of the body and glaze composition are consistent, the tiles being almost free of corrosion. In the case of the analysis of the corrosion products occurred on the metallic artifacts, the lighter elements could not be estimated due to the varied corrosion products.

The measurements of the body were iterated less than the glaze layer due to the consistency of the homogeneous paste composition. The glaze had to be measured several times, in different spots because of the heterogeneous structure of the ancient ceramic glazes originating from the complexity of the decor (that impose very variable concentration of colouring agents), the firing conditions and constraints due to the thinness of the coating. Further, undissolved and/or dissolved minerals/pigments in the glaze cause discrepancies of the analyses. The distribution of both varied and unvaried measurements of the transparent glaze layer as well as the coloured glazes can be explicitly seen in Fig. S3 with the example of Pb vs. Si plot. The lines in the figures of scatter plots are drawn as a guide for eyes. Elements issued from single raw material in variable proportion in the glaze, for instance, the colour precursor, network modifiers and fluxing agents of the glaze, will be located on a linear curve starting from the origin [25,31]. If the element remains undissolved in the glaze of which the thickness varies, the contribution of the substrate will affect the measurement of the glaze composition. Therefore, a statistical approach comes into prominence for the glaze analyses. When an element dissolves in the vitreous matrix of the glaze, it can be considered that whatever the measurement, it will remain constant and the points will be aligned horizontally or vertically depending on the choice of axes.

A statistical program, titled Minitab 17, was used for drawing graphs of PCA (principal component analysis) and dendrogram which shows the similarity and differences in the body compositions of the tiles allowing an easy interpretation for archaeologists and researchers not expert in the ceramic technology.

### **3. Results**

#### **3.1. Body**

Before the measurement with the pXRF, a visual examination was performed to identify the colour changes in the paste. When we compared the colours visually, three types of paste were determined, in red, light beige and white colours. In the same atmospheric conditions

during the firing process, a high addition of limestone in the body clarifies the colour of the paste from red to yellow, and when it is added in low quantity, the colour of the body turns to red with the same iron content. Alumina ( $\text{Al}_2\text{O}_3$ ) versus quartz ( $\text{SiO}_2$ ) scattering plot (Fig. 2 upper) confirms the use of different raw materials in the body composition of the tiles, varying from the production period. However, high alumina content indicates the addition of a high amount of alumina-rich clay and high silica content showing a high level of quartz grains.

In addition to the visual examination, the elemental analysis concluded that three groups of body composition were defined with the pXRF measurements, as follows:

- i- *Group #1:* 14th-15th-centuries productions contain a low amount of quartz (around 50 %  $\text{SiO}_2$ ) and high alumina (12-16 wt%  $\text{Al}_2\text{O}_3$ ) which means the use of a clay-rich paste. Studies on the early period productions of Iznik confirms the results of Group #1 [8,16-18] and linked this production to Timurids production.
- ii- *Group #2:* 16th-17th-centuries productions contain a high amount of quartz (65-85 %  $\text{SiO}_2$ ) and low alumina (3-6 wt%  $\text{Al}_2\text{O}_3$ ): a typical fritware recipe well established for "Iznik" tiles [8,9,11,18,37-39].
- iii- *Group #3:* A third group including the tiles B8-1 (assigned 16th-century), B7-8 (second half of 16th-century), and B7-7 (17th century) have low content of  $\text{Al}_2\text{O}_3$  (3.6-6.3 wt%), a medium level of  $\text{SiO}_2$  (39-62 wt%) and an additional amount of calcium (27.5 wt% in the body of B8-1, 37.2 wt% in B7-7, and lower amount in B7-8, 11 wt% CaO) which represents the presence of a calcareous paste rather than a siliceous – clayey body (see Fig. 2).

Comparison between present pXRF measurements (solid labels) and measurements made at the laboratory with fixed advanced instruments (specific labels) in Figs. 2 & 3 will help to assess the reliability of pXRF vs. Analyses at the Laboratory. The scatter plots of K/Si versus Ca/Si (Fig. 2 middle) and Ca versus Fe (Fig. S4) confirm the above classification. The tiles B7-8, B8-1, and B7-7 from Group #3 have the same amount of potassium, but with changing amount of calcium. This result reveals the use of a mixture of two different raw materials, one bridging calcium (marl or limestone?) and the other potassium (frit?). Sodium content in the body and glaze composition was calculated from the remaining amount of the sum of the other elements and plotted in scatter diagram (see Fig. S4 middle and Fig. S5 bottom). The sum of  $\text{Na}_2\text{O}$  (sodium oxide) and  $\text{K}_2\text{O}$  (potassium oxide) refers to the content of the alkalis in ceramic bodies and glazes. The body analyses confirmed the three groups which are rich in alkalis (Group #1), rich in lead-alkali (Group #3) and poor in alkalis (Group #2).

A statistical approach, which allows the archaeologists to a better interpretation of the results, is adopted by a graph of dendrogram (See Fig. 2 bottom) which shows the similarities of the shards regarding their body composition. This graph clearly demonstrates two tiles (B8-1 and B7-7) of Group #3 are very different than the Groups #1 and #2. B7-8 is also in the same group but closer to the Group 2 in terms of the body constituents. This

dendrogram confirms the findings carried out by the scientific analyses. The scatter plot of Ca versus Fe (Fig. S4 upper) shows that the earlier productions contain much more iron but less calcium which also evidences the red colour of the body. The visual examination differentiated the pastes in off-white (or light beige) colour in which the analyses found a high content of calcium with very low amount of iron representing the Group 3. In the group #2, there are two sub-groups which differ in terms of the preparation of the raw materials. One may correspond to the purification of the clay of Group #1 by removing the iron content by washing or selection.

A similar classification to the dendrogram can be obtained by using the PCA method (see Fig S4 bottom). The scatter plots of the body and glaze constituents are more efficient for the interpretation of the results but require an intense knowledge of the ceramic technology. However, the use of PCA and similar statistical methods (e.g. dendrograms) will be more comprehensible for the archaeologists and researchers less expert in the ceramic production technology.

Comparison between present pXRF measurements (solid labels) and measurements made at the laboratory with fixed advanced instruments (specific labels) in Figs. 2 & 3 confirm the validity of non-destructive measurement with XRF pistol.

### 3.2. Glaze

#### Tin/lead ratio

Fig. 3 (upper) represents the distribution of tin versus lead normalized by silicon content measured in the transparent glaze or the glaze having the white decor beneath. Tin content varies between 0.06 and 6.26 wt% (0.072-7.95 wt% SnO<sub>2</sub>) and lead is found between 21 and 42 wt% (23-46 wt% PbO). The values of the ratio of tin versus lead measured on the glazed shards of this study are given in Table S3, (Supplementary Materials) with the comparison of the literature [11,14,25,27]. Lines coming from the origin at zero have been drawn intentionally as an eye guide for the easier interpretation of the results. The scatter plot of Sn/Si versus Pb/Si shows three different groups which justify the decrease in the use of tin oxide by centuries. The lines show that the tiles were made with two Pb-Sn sources but varying in quantity added. Tin mining places are rare making the cost of tin high, and it seems reasonable that potters limit the Sn content. Sn can be also associated to Pb, in particular if bronze waste are used (ref). These three groups defined by tin to lead ratio correlate with the groups determined by the analyses of the body composition. We note only two exceptions: A7-4 from Group #1 and B7-3 from Group #2 are not included in the scatter plots of the glaze components because they were not glazed. Comparison between present pXRF measurements (solid labels) and measurements made at the laboratory with fixed advanced instruments (specific labels) in Figs. 2 & 3 confirms the validity of data collected with portable instruments.

Group #1 (first productions, 14<sup>th</sup>-15<sup>th</sup> centuries) shows two glaze technologies, one with high amount of tin and lead (B7-1: 7.95 wt% SnO, 32.5 wt% PbO; A7-3: 4.93 wt% SnO, 33 wt% PbO) already observed [25] and the other without tin (B8-0: 0.15 wt% SnO<sub>2</sub>) but with the highest amount of lead (46 wt% PbO). More statistic needed to exclude that this sample is nor representative (waste). All the shards of Group #2 have a similar amount of lead and tin, except B7-2. The lead content in the glaze of B7-2 is in the same range of Group #2, but the tin amount is higher than the other tiles of the group. With regard to tin content, B7-2 is closer to Group #1. The group #3 is divided into two subgroups, B8-1 and B7-8 having a considerable amount of tin, and B7-7 with low tin probably coming as the impurity of the lead source.

The production of the second half of 16th-century is generally the most controlled technology of Iznik provenance showing a slight variation of the glaze composition (Fig. 3 upper) [19]. Only the tiles B7-10 and B7-15, in the characteristic manner of polychromic Iznik productions, contain a very low amount of tin (0.05 wt% and 0.52 wt% respectively).

The 16th and 17th-centuries productions detected as clustered in the lower part of the Sn/Si versus Pb/Si scatter plots (Fig. 3 upper) representing the lowest content and small variation of tin (0.2-0.5 wt% SnO<sub>2</sub>) with more extensive distribution of lead (22-45 wt% PbO).

Pb/Si versus Mg/Si scatter plots (Fig. 3 bottom) confirm the distribution of the three groups, typically. Group 1 and the subgroup 3<sup>2</sup> have a higher amount of Mg and Pb while Group #2 and subgroup 3<sup>1</sup> are clustered together in the low Mg/Si region. The straight line drawn from the origin indicates that the frit brings both lead and magnesium. The brown layer (F1) is a formation of the glaze on the clays of the kiln walls which is aligned on the line coming from the origin and closer to B7-1.

The amount of sodium is calculated for the glaze composition, as we did on the body, and plotted in the scatterplot of alkali content versus lead oxide (Fig. S5 bottom). The dispersion of the results is broader than the body content because the thickness of the glaze varies and also the penetration depth of X-rays changes resulting the influence of the body content in the glaze analysis. This graph evidence mainly the presence of two types of glazes, alkali-rich lead (B8-0, A7-3 of Group #1 and B7-7 of Group #3) and lead-rich alkali (rest of the Groups 1, 2, 3) in the studied shards with changing amount of tin in the glaze (Fig. 3 upper).

The detection of bismuth with the pXRF may give valuable information about their use in specific tile production and the source of lead which could allow the identification of the provenance of the raw materials. Bismuth has already detected in the transparent glaze of some Ottoman tiles [18,25]. Fig. 4 upper shows that bismuth is an impurity of lead. However, bismuth can also be an impurity of a cobalt source. Therefore, the amount of bismuth should be compared both in white and blue areas. The analysis showed that bismuth is extracted from the glaze not from the blue colouring agent in the tiles A7-1, A7-2, B7-2, B7-7, B7-9, B7-10, B7-11, B7-16, and B8-3. The other tiles (B7-4, B7-5, B7-6, B7-8, B7-

12, B7-14, B7-15, B7-17, and B8-2) having the blue areas contain (also?) bismuth as an impurity of cobalt source. The scatter plots of K/Si vs. Ca/Si (Fig. 4 bottom) show mainly two different types of fluxes used in the glaze, some containing only potassium, and the others having potassium and calcium, according to the literature [40].

In the scatter plots of Al versus Si (Fig. S5 upper), the tiles of 14th-15th-centuries are aligned together with less amount of silicon. For the tiles of the group 1, aluminium is an impurity of sand. The tiles of the groups #2 and #3 clustered as the second group of the plot. The tiles of second half of the 16th-century contain a low amount of aluminium and high amount of silicon which is typical for the classical period of Iznik production.

#### On-site kiln wall measurement

An on-site measurement was carried out to identify the glassy green material formed on the walls of the fourth kiln (see Fig. S2). The analysis showed that this glassy surface surprisingly contains almost no lead (0.047 wt% Pb) but a high amount of sulphur (4.313 %wt). Throwing *alquifoux* (PbS) inside the kiln at the end of the firing process is a classical technique which was used in Morocco for the traditional pottery production, in these days [41,42]. This knowledge may explain the presence of sulphur. As lead vaporizes easily, it does not leave any residue on the wall inside the kiln, the condensation of lead being further (chemney). The other elements found on the surface are Mg (3.20 wt%), Al (4.44 wt%), Si (18.68 wt%), P (0.317 wt%), K (3.22 wt%), Ca (13.42 wt%), Ti (0.79 wt%), Cr (0.05 wt%), Mn (0.15 wt%), and Fe (6.83 wt%).

### 3.3. Colouring agents

#### Blue colour

Three types of cobalt were identified in the blue decors of the tiles studied (see Fig. 5 upper).

- i) No arsenic containing tiles: A7-1, A7-2, B7-2, B7-4, B7-5, B7-6, B7-7, B7-8, B7-9, B7-10, B7-11, B7-12, and B8-3
- ii) Constant arsenic content: B7-3 (and B8-2 ?)
- iii) Constant cobalt: B7-14, B7-15, (and B8-2 ?) and B7-17

Bismuth was detected in the blue decors of all the shards except B7-3 which was not glazed but painted (see Fig. 5 middle). This suggests that bismuth may be an impurity of the lead source, and not a trace element of cobalt found in the blue decor. When compared the bismuth amount in the transparent glaze to the blue decor, it is detected that two different types of cobalt exist in the blue decors. One group contains bismuth and the other does not contain. It is found that bismuth is present only in the glaze of A7-1, A7-2, B7-2, B7-7, B7-9, B7-10, B7-11, B7-16, and B8-3. The blue decors which contain bismuth as an impurity of

cobalt belong to the tiles B7-3, B7-4, B7-5, B7-6, B7-8, B7-12, B7-14, B7-15, B7-17, and B8-2. The scatter plots Mn/Si versus Co/Si and Co/Si versus Ni/Si (Fig. S6) shows the use of different cobalt sources. The arsenic-rich decors are also rich in nickel (B7-3, B7-17). Moreover, the tiles B8-3 and B7-2 are rich in manganese which contain no arsenic.

#### Red colour

Fig. S7 upper left shows the content of Fe and Cu in the red decor. The two tiles of 17th-century (B7-14 and B8-3) contain both iron and copper in the red colour. For the other tiles, which correspond to the productions of 16th and second half of the 16th-centuries, iron may be an impurity rather than the deliberate addition. Up to know, only a mixture of quartz and hematite (Armenian bole [19,24]) or a silicate mineral called aegirine ( $\text{NaFe}^{3+}(\text{Si}_2\text{O}_6)$ ) [11,26] was recognized in the red areas of Iznik productions, but for the first time, this study showed that the artist might potentially use the mineral of bornite ( $\text{Cu}_5\text{FeS}_4$ ) which was found vastly in Anatolia in 16th-17th centuries, for decorating in red colour. Only for the tiles B8-3, A7-1, and B7-10, there exist a diffusion of copper towards the red area from the adjacent green/turquoise colour which was observed from the spot images of the pXRF instrument. For the tiles B7-14 and B8-3, the amount of iron is very high regarding the other tiles (averagely 1.8 wt%). The copper content varies between 0.1 – 0.3 wt % with about 0.4- 0.6 iron for the other tiles.

#### Turquoise colour

The similar scatter plots (Fe/Si versus Cu/Si) are drawn for the turquoise colour (see Fig. S7 upper right). Consequently, a mixture of iron and copper detects for the tiles of 14th-15th centuries (B7-1 and A7-3). However, the main turquoise colourant for the other tiles is copper and iron is found as an impurity.

The scatter plots of Cu/Si versus Fe/Si (Fig. S7 bottom left) and Cu/Si versus Cr/Si (Fig. S7 bottom right) were drawn to identify the composition of the green coloured areas. Two types of green pigments were determined; chrome and copper are containing. The green decor of the tile B7-16 and B7-17 contain chrome-based pigment while the other tiles have different ratios of copper depending on the light and dark colours. The tiles B7-14 and B7-16 do not contain any iron with copper, but the other tiles do.

#### Black lines

The black lines are measured for the tiles A7-1, A7-2, B7-9, B7-14, B7-15, B7-16, and B8-3. Chrome containing pigment is found only in the line decors of B7-14 (0.35 wt% Cr), B7-15 (0.6 wt%), and B8-3 (0.16 wt%). The same tiles contain a higher amount of iron. It is clearly seen that an iron-chromate spinel was used in the black lines of these tiles. The other shards, A7-1, A7-2 B7-9, and B7-16 contain only iron in the black lines.

## 4. Discussion

## Validity of non-destructive elemental analyse with portable instrument

On-site measurements with portable instruments become crucial in terms of the reproducibility and reliability of the results obtained. The accuracy of the data obtained with the pXRF can be provided by using the proper calibration standard which allows doing a semi-quantitative analysis for determining the composition of the body, glaze, and pigment used in the decor. In this study, pXRF results of the tiles were compared to the past analyses of the Iznik kiln excavation materials carried out with SEM-EDS in the laboratory conditions by plotting all the data in the same scatter plots (see Fig. 3 for the body, Fig. 5 for the glaze) [2,28,29]. The tiles having the red body, which were assigned as the earlier productions of Iznik are grouped with Group #1, which concerns the 14th-15th-centuries productions (see Fig. 3). The stone-paste type, which is the productions of the classical Iznik period, from 16th-century, are grouped with the similar type of shards having more quartz and less alumina in the body. Only the group 3 which includes the monochrome green tile B8-1, polychrome tile of classical Iznik period (2nd half of the 16th-century) B7-8, and the tile with Kaaba figure B7-7 are grouped separately in comparison with the past measurements. The reason that the pXRF and laboratory measurements could well plot in the same scale is comforted by the use of the same glass (e.g. Corning Brill B, C, D, NIST SRM 611) and geological reference standards (e.g. red mud, diorite DR-N) during the calibration of the pXRF and laboratory type instruments [43,44].

## Monochrome to polychrome tiles

The tile production in the Anatolian territories, which was trademarked as Ottoman and/or "Iznik" was divided into four phases between 12th- and 17th-centuries [40]. The phases include 1) the period of Anatolian Seljuks during 12th-13th-centuries with the importation of Persian techniques, where the most representative tile ornamentation covered the walls of Gök Medrese in Sivas, 2) occasional production of the tiles in the early 14th-century by potters who were using the technology of lead-glazed earthenware with red clay in the body, 3) period of Masters of Tabriz in the early 15th-century, and 4) after a gap in tile production in the late 15th-century of some thirty years, re-beginning of the tile production in the 16th-century in Iznik kilns [40,45]. Unfortunately, the workshops, where the Seljukian and Persian craftsmen worked, unrecorded as well as Timurid potters who got artistic influences by the Chinoiserie style [45]. The only evidence of the group of Masters of Tabriz is their signature on the tilework of the Yeşil mosque and tomb of Mehmed I (1419-1424) in Bursa still without any knowledge of the production place of these tile revetments. The literature on the Ottoman ceramic art states that had a similar technique applied in the Muradiye Mosque at Edirne, in which believed that the same group members had worked [45]. Notwithstanding, the studies on Muradiye tiles showed that two different technologies had used in the polychrome tiles of the *mihrab* and blue-and-white tiles on the side walls [25]. The technology of the (polychrome) tiles of the *mihrab* is related to Timurid and Seljuk heritage while the blue-and-white tiles are particular productions like Üç Şerefeli Mosque

tiles studied in that research [25]. Primarily, the study of the 14th-15th centuries tiles is crucial in the investigation of the transition/link between Anatolian Seljuk and Ottoman ceramic production technologies. Therefore, some earlier Iznik's productions picked, dating back between 14th-15th centuries to identify the technology used in the body and glaze. Additionally, the tiles of the classical period of Iznik (16th- and the second half of the 16th-century), as well as the later productions, were analysed during this preliminary study of the one-day campaign. Because of the time-bound, the number of the tiles analyzed with pXRF was confined to the different representative technologies of Iznik tiles. The selection criteria were based on the presence of glaze, polychromic and monochromic decors and different patterns are drawn. Three glazed tiles painted with the main colour lines, where the artist might try to find the best saturation and hue of red, green, and blue colours, were included in this preliminary study to compare the colouring pigments with the coloured areas of the other tiles' decors. Additionally, one shard in biscuit form, where the paste recipe was defined as a representative technology of the monochrome glazed tiles of 14th and 15th-centuries, and one painted but not glazed shard analyzed.

### Body

Evliya Çelebi, in his book (*Seyahatname*), states that around three hundred ceramicists worked in the workshops of Iznik [33]. Recent excavations also showed that almost thirty tile kilns were explored in the last years [46]. The technology of the Seljukian tiles having a black decor under the turquoise glaze has been encountered in the excavations of Iznik. The technique had used from 14th-century for a long time in the production of daily use ceramics. The body colour of the tiles and ceramics is usually ash yellow in the Seljuk period, reddish in Beylic and early Ottoman period, and dirty white during the classical period of Ottoman era [32]. When compared the body composition of the tiles from 14th-15th-centuries (B8-0, B7-1, A7-4, A7-3) with the literature [14,47], not any similarity detected with the Persian technology during both Seljuk (1050-1200 AD) and Timurid (1400-1440 AD) periods. The Damascus production in Syria during the Mamluk period (1250-1350 AD) is closer regarding the calcium content, but alkali amount is still less than the tiles of the Group 1 [14]. However, Group 1 tiles have a similarity with the tiles 82, 83 from Yeşilce Mosque (Edirne) and Syrian productions regarding the body which is composed of higher content of calcium, iron, and aluminium which differs in technology from the other tiles studied in this research [25,47]. Typical 16th-century productions of Iznik are consistent with the documented tiles of Selimiye Mosque which represents the most successful period of Iznik workshops [25].

### Tin oxide

The use of tin oxide in the glaze decreases through centuries which may have been caused by the high costs of tin and by the perfect mastery of the white quartz slip. Fig. 6 upper features the distribution of Sn/Pb ratio representing the different groups and compared with the literature including past measurements carried out on Ottoman tiles, "Iznik" tiles at

Edirne, Fatimid, Seljuk, and Timurid tiles [11,14,25,27]. The tin content of 16th-17th-centuries productions are similar to the Ottoman reference tiles from 16th- and 17th-centuries according to the homogeneity of production at that period [19,20]. Earlier productions of Iznik, namely Group 1, tin-rich, are closer to the Seljukian tiles. B8-0 of the group 1 from 14th-15th centuries evidences an inconsistency of the tin content in the glaze, as well as B8-1 of 16th-century (Group 3) and B7-2 of 17th-century (Group 2). Tin content of B8-0 is found lower than expected, and for B8-1 and B7-2, it is found higher. The tiles of the classical period of Iznik (2nd half of the 16th-century) have a similar amount of tin, except the tile B7-10. The workshop, where it was produced or the period may differ for B7-10. Studied samples being kiln waste, wrong artefact is possible.

### Colouring agents

The tiles B7-11, B7-12, and B7-13 may be a study collection of the potter(s), where he/she tried to define the hue of the main colours, green, blue and red. He might also tried to define the best recipe of the paste suitable with the decor and glaze because the body composition varies in these three shards mainly with respect to potassium, calcium, and lead content which may reflect the use of lime-alkali (B7-13) and lead-rich frit (B7-11) in the paste. The analyses of the coloured areas, especially red and blue decors, showed that the composition is stable reflecting a controlled production process. Indifferences in the blue and red area measurements may be due to the higher thickness of the glaze under, where the penetration depth of X-rays does not reach so much toward the coloured area. A similar diagnostic had come across on the red pigments of the classical period of 16th-century. Iznik productions well-known with the famous red pigment in which hematite (Armenian bole, an intimate mixture of hematite and quartz) was added [19,26]. However, the pXRF measurements found some iron with copper addition. Only, in the decor of B8-3, A7-1, and B7-10, the diffusion of copper may occur from the pollution of the adjacent colours across the red area. With the addition of  $\text{Cu}_2\text{O}$ , a dull-red obtained while the use of metallic copper nanoparticles leads to a bright red. The investigation of the pigments found in the red areas with high-resolution instruments (e.g., micro-XRF, micro-XRD, SEM-EDS, Raman and TEM, on polished sections) can justify the presence of copper with hematite.

### Cobalt origin

Mainly, three sources of cobalt applied with pigments in the blue decors of archaeological ceramics. 1) European cobalt: the mixture of Co-Ni-Fe-As, 2) Asian cobalt: the mixture of Mn-Co-Fe, no As, 3) Kashan (Persian) cobalt: Co with a high amount of As, Fe; no Ni, Cu, Zn [48-56]. Constantinescu mentioned that Porter, a researcher on the Islamic art, stated the use of Erzgebirge (European source) cobalt ores and added that a change in the composition of the blue glazes was observed in 1520 by the presence of As and Bi by reduced amounts of Fe and Ni [15].

Three types of cobalt were determined with the measurements of the pigments present in the blue areas depending basically on the arsenic content: no arsenic, constant arsenic and **mixture**. The detailed analysis showed that the blue decors of the tiles B7-3, B7-14, B7-15, B7-17, and B8-2 contain a mixture of Co-Ni-Fe-As which is consistent with the use of European cobalt source. Ni is only rich in As-containing blue areas. Additionally, copper was also detected. These tiles belong to the Group 2 and are dated back to the 16th-17th centuries productions. Any Persian cobalt source was not used in the blue areas because the Kashan cobalt is expected to contain a high amount of As and Fe with no traces of Ni, Cu, and Zn. Thus, it may be assumed that the Persian influence did not affect the choice of the raw materials used in the tiles but the technology only.

The blue decors with Fe, Cu and without As content is divided into two types:  $Mn/Co < 1$  and  $Mn/Co > 1$ . The two tiles of the group 3 (B7-8 and B7-7) and the tiles from the group 2 (B7-4, B7-5, B7-6, B7-9, B7-16, and A7-1) sorted in the group of  $Mn/Co < 1$ . When compared to the literature, the cobalt source could not be defined for this group ( $Mn/Co < 1$  without As). Three tiles of the group 2 from 2nd half of 16th- and 17th-centuries, B7-10, B8-3, and A7-2 contain  $Mn/Co > 1$  (1.38, 2.57, 2.6 respectively) which may be related to the Chinese cobalt source used in the late Ming dynasty at Jingdezhen, where no arsenic was detected and  $Mn/Co > 3$  [57].

Figure 6 bottom shows the ratio of cobalt versus manganese of the analysed artefacts and triple diagram of Co, Ni, Mn normalized by Si (Fig. 5 bottom) with the comparison of the reference data collected from the blue decors, where the pigments are originated from Chinese, Persian and/or European pigment sources [58-65]. The triple diagram shows three groups of blue decors. The main group of the tiles studied in this research clustered in Group #3 with the reference materials of Şah Melek Paşa and blue and white tiles of Muradiye Mosque at Edirne [25]. B7-4 and A7-1 plotted at the intersection of the Group 2 and 3 with the reference material of Selimiye Mosque (Edirne). These groups do not refer to the groups that were already defined by the measurement of the body. The numbers are specifically attributed to the scatter plots of the ternary diagram in Fig 10. B7-16, B7-9, and B7-10 are at the intersection of Group #1 and #3 while B8-3 and A7-2 are plotted closely in Group #1 with the reference tiles of Üç Şerefeli Mosque [25].

## 5. Conclusion

This preliminary study on the tiles excavated at Iznik kiln site shows the efficiency of the pXRF instrument. When compared to the previous measurements carried out with SEM-EDS at the laboratory, the portable system has an equivalent detection capability in discriminating different groups of the tiles regarding their body, glaze and decor compositions **even Na could not be measured with the pXRF which influence the alkali content found in both glaze and body.** a reasoned selection of parameters related to ceramic raw materials appears to be more effective than blind PCA analyse.

The past studies have shown that earlier periods of Iznik productions contain clayey bodies and later the stone-paste / fritware technology was introduced with 80% of quartz, 10 % of clay and 10 % of lead-rich frit in the paste [11]. However, in this study, a new type of paste is evidenced for Iznik tiles, which are calcium-rich. Our study encountered, also, with different glaze technologies because the change of the body composition imposes. The thermal expansion is very dependent of the quartz content due to the alpha-beta transition during the firing process [66]. Different cobalt ores, European (Co-Ni-Fe-As), Chinese (Mn/Co > 1, no As) and an unknown source (Mn/Co < 1, no As) were identified. Mixture of cobalt from different sources is demonstrated. **The study discovered one new evidence on red pigment. Two types of red pigments were detected, iron-containing, and a mixture of iron and copper.**

### **Acknowledgments**

Noyan Özdemir from TROY-MET (Istanbul) is gratefully acknowledged for making Hitachi X-MET 8000 Expert Geo pXRF instrument available in Iznik for on-site measurements. The authors thank Yurdanur Akpınar for providing the coordination between the authors.

## References

1. O. Aslanapa, S. Yetkin, A. Altun, İznik çini fırınları kazısı: II. Dönem 1981-1988, İstanbul: Tarihi Araştırmalar ve Dokümantasyon Merkezleri Kurma ve Geliştirme Vakfı, 1989.
2. T. Tulun, G. Doner, F. Calisir, N. Cini, N. Karatepe, A. Mericboyu, A. Tekin, A. Altun, B. Arli, H. Arli, An archaeometric study on ancient Iznik ceramics, BAU Fen Bil. Enst. Dergisi 4 (2) (2002) 34-43.
3. B. Demirsar Arlı, Evaluation of Iznik tiles examples from Iznik tile excavation, Journal of History Culture and Art Research 7 (1) (2018) 578-594.
4. R.M. Riefstahl, Early Turkish tile revetments in Edirne, Ars Islamica Vol. 4, Freer Gallery of Art, The Smithsonian Institution & Department. of the History of Art, University of Michigan, 1937, pp. 249-281.
5. G. Necipoglu, From International Timurid to Ottoman: A change of Taste in Sixteenth-Century Ceramic tiles, Muqarnas 7 (1990) 136-170.
6. Ş. Yetkin, Anadolu'da Türk Çini Sanatının Gelişmesi, İstanbul Üniversitesi Edebiyat Fakültesi Yayınları No.1631, İstanbul, 1986.
7. A. Lane, The Ottoman pottery of Iznik, Ars Orientalis 2 (1957) 247-281.
8. J. Soustiel (Ed)., La Céramique Islamique — Le Guide du Connaisseur, Office du Livre — Editions Vilo: Paris, 1985.
9. N. Atasoy and J. Raby, Iznik: The Pottery of Ottoman Turkey, London: Alexandria Press, 1989.
10. W. B. Denny, Iznik La Céramique Turque et l'Art Ottoman, Citadelles and Mazenod: France, 2004.
11. G. Simsek, Characterization of structure of alkali and lead-alkali glazes by Raman spectrometry, PhD Thesis, Istanbul Technical University, 2011.
12. D.W. Kingery, D. Smith, In Ancient Technology to Modern Science, Vol. I, Ceramics and Civilization, Kingery DW (Ed). American Ceramic Society: Columbus, OH 1984; 273.
13. M.S. Tite, Iznik pottery: An investigation of the method of production, Archaeometry 31 (2) (1989) 115-132.
14. M.S. Tite, S. Wolf, R.B. Mason, The technological development of stonepaste ceramics from the Islamic Middle East, J. Archaeol. Sci. 38 (2011) 570-580.
15. B. Constantinescu, D. Cristea-Stan, I. Kovács, Z. Szökefalvi-Nagy, External milli-beam PIXE analysis of the mineral pigments of glazed Iznik (Turkey) ceramics, Period. Mineral. 83 (2) (2014) 159-169.

16. J. Henderson, Iznik ceramics: a technical examination. In N. Atasoy and J. Raby, Iznik: The Pottery of Ottoman Turkey (Ed. Y. Petsopoulos). London: Alexandria Press, 1989, pp. 65-70.
17. J. Raby, Part 2: 1480-1560: development and growth of Iznik pottery. In N. Atasoy and J. Raby, Iznik. The Pottery of Ottoman Turkey (Ed. Y. Petsopoulos). London: Alexandria Press, 1989, pp.50-64.
18. L. Martinet, A. Ben Amara, C. Pacheco, Q. Lemasson, B. Moignard, L. Pichon, Ph. Colomban, Colored Glaze Tiles during the Ottoman Empire (beginning of the 15th to the/ mid 16th century)? EMAC 2015 Proc., 13th European Meeting on Ancient Ceramics, 24-26th September 2015, Athens.
19. Ph. Colomban, V. Milande, L. Le Bihan, On-site Raman analysis of Iznik pottery glazes and pigments, J. Raman Spectrosc. 35 (2004) 527–535.
20. Ph. Colomban, R. de Laveaucoupet, V. Milande, On Site Raman Analysis of Kütahya fritwares, J. Raman Spectrosc. 36 (9) (2005) 857-863.
21. S. Demirci, E.N. Caner-Saltik, A. Turkmenoglu, S. Ozçilingir-Arkun, O. Bakirer, Raw material characteristics and technological properties of some glazed ceramics and tiles in Anatolia, Euro Ceramics VIII, PTS 1-3, Key Engineering Mater. 264-268 (1-3) (2004) 2395-2398.
22. M. Özçatal, M. Yaygingöl, A. Issi, A. Kara, S. Turan, F. Okyar, S. Pfeiffer Tas, I. Nastova, O. Grupce, B. Minceva-Sukarova, Characterization of lead glazed potteries from Smyrna (Izmir/Turkey) using multiple analytical techniques; Part I: Glaze and engobe, Ceram. Int. 40 (2014) 2143-2151.
23. E. N. Caner Saltık, Ph. Colomban, V. Soulet, S. Demirci, A. Türkmenoğlu, S. Özçilingir Akgün, Ö. Bakirer, Analyses of Anatolian medieval ceramic glazes using XRD and non-destructive Raman micro-spectrometry, Colloque du GMPCA, Archaeometrie 2013, Bordeaux, 16-19 April 2013.
24. G. Simsek, Ph. Colomban, V. Milande, Tentative differentiation between Iznik tiles and copies with Raman spectroscopy using both laboratory and portable instrument, J. Raman Spectrosc. 41 (5) (2010) 529-536.
25. G. Simsek, O. Unsalan, K. Bayraktar, Ph. Colomban, On-site pXRF analysis of glaze composition and colouring agents of “Iznik” tiles at Edirne mosques (15th and 16th-centuries), Ceram. Int. 45 (2019), 595-605.
26. G. Simsek, A.E. Geckinli, An assessment study of tiles from Topkapi Palace Museum with energy-dispersive X-ray and Raman spectrometers, J. Raman Spectrosc. 43 (2012) 917-927.
27. A.E. Geckinli, G. Şimşek, Topkapı Müzesi Deposunda Bulunan Seramiklerin Tanımlanması, Unpublished report, 2011.
28. F. Okyar, Characterization of Iznik Ceramics, PhD Thesis, Istanbul Technical University, 1995.
29. S. Paynter, F. Okyar, S. Wolf, M.S. Tite, The production of Iznik pottery – A reassessment, Archaeometry 46 (3) (2004) 421-437.

30. M.S. Tite, A.J. Shortland, N. Schibille, P. Degryse, New Data on the Soda Flux Used in the Production of Iznik Glazes and Byzantine Glasses”, *Archaeometry* 58 (1) (2016) 57-67.
31. G. Simsek, F. Casadio, Ph. Colomban, K. Faber, L. Bellot-Gurlet, G. Zelleke, V. Milande, E. Moinet, On-site identification of earlier Meissen Böttger red stonewares using portable XRF: 1, body analysis, *J. Am. Ceram. Soc.* 97 (9) (2014) 2745-2754.
32. G. Oney, Z. Cobanlı, Anadolu’da Türk devri çini ve seramik sanatı, Ankara : Kültür ve Turizm Bakanlığı, 2007.
33. A. Altun, J. Carswell, G. Oney, Sadberk Hanım Müzesi Türk Çini ve Seramikleri, Vehbi Koç Vakfı: İstanbul, 1991.
34. B. Demirsar Arlı, A. Altun, Anadolu Toprağının Hazinesi Çini: Osmanlı Dönemi, Kale Grubu Kültür Yayınları: İstanbul, 2008.
35. J. Carswell, Iznik Pottery (Eastern Art), Interlink Pub Group Inc, 2006.
36. A. Seyfarth, Boron in glass determination using WDXRF, *Adv. X-Ray Anal.* 51 (2008) 269-274.
37. Ch. Kiefer, Les Céramiques siliceuses d'Anatolie et du Moyen-Orient. *B. Soc. Fr. Ceram.* 30 (1956) 3-24.
38. Ch. Kiefer, Les Céramiques siliceuses d'Anatolie et du Moyen-Orient. *B. Soc. Fr. Ceram.* 31 (1956) 17-34.
39. Ch. Kiefer, La Céramique Islamique — Le Guide du Connaisseur, J. Soustiel (ed), Office du Livre — Editions Vilo: Paris, 1985, 368.
40. J. Henderson, J. Raby, The technology of fifteenth century Turkish tiles: an interim statement on the origins of the Iznik industry, *World Archaeol.* 21 (1) Ceramic Technology, Taylor & Francis, Ltd. (1980), pp. 115-132.
41. Wiktionnaire, Definition of alquifoux, retrieved from <https://fr.wiktionary.org/wiki/alquifoux>, on November 13rd, 2018.
42. M-C. Bailly-Maitre, N. Minvielle Larousse, E. Kammenthaler, T. Gonon, G. Guionova, L’exploitation minière dans la vallée du Chassezac (Ardèche), *Archaeologie médiévale*, 43 (2013), 47-76.
43. J. Burlot, Premières productions de céramiques turques en Anatolie occidentale : Contextualisation et études techniques, PhD Thesis, Université Lumière Lyon 2, 2017.
44. P. Kuisma-Kursula, Accuracy, Precision and Detection Limits of SEM-WDS, SEM-EDS and PIXE in the Multi-Elemental Analysis of Medieval Glass, *X-Ray Spectrom.* 29 (2000), 111-118.
45. L. Golombek, Timurid potters abroad, *Oriente Moderno* 15[76], N°2 La Civiltà Timuride come fenomeno internazionale vol II (Letteratura-Arte), (1996) 577-586.
46. S. Satir, Türk kültüründe İznik çinilerinin önemi ve güncel değerlendirilmesi, 8. ICANAS (Uluslararası Asya ve Kuzey Afrika Çalışmaları Kongresi) Bildiri Kitabı, Ankara: Atatürk Kültür, Dil, Tarih ve Yüksek Kurumu, 2008, 1129-1144.

47. M. Tite, O. Watson, T. Pradell, M. Matin, G. Molina, K. Domoney, A. Bouquillon, Revisiting the beginnings of tin-opacified Islamic glazes, *J. Archaeol. Sci.* 57 (2015) 80-91.
48. M. Matin, A. M. Pollard, From ore to pigment: A description of the minerals and an experimental study of cobalt ore processing from the Kashan mine, Iran, *Archaeometry*, 59 (4) (2017), 731-746.
49. R. Wen, The cobalt blue pigment used on Islamic ceramics and Chinese blue-and-white porcelains, PhD Thesis, University of Oxford, 2012.
50. C. Viti, I. Borgia, B. Brunetti, A. Sgamellotti, M. Mellini, Microtexture and microchemistry of glaze and pigments in Italian Renaissance pottery from Gubbio and Deruta, *J. Cult. Herit.* 4 (2003), 199-210.
51. F. Casadio, A. Bezur, K. Domoney, K. Eremin, L. Lee, J. L. Mass, A. Shortland, N. Zumbulyadis, X-ray fluorescence applied to overglaze enamel decoration on eighteenth- and nineteenth-century porcelain from central Europe, *The International Institute for Conservation of Historic and Artistic Works* 2012.
52. S. Coentro, J. M. Mimoso, A. M. Lima, A. S. Silva, A. N. Pais, V. S. F. Muralha, Multi-analytical identification of pigments and pigment mixtures used in 17th century Portuguese azulejos, *J. Eur. Ceram. Soc.* 32 (2012), 37-48.
53. I. Borgia, B. Brunetti, I. Mariani, A. Sgamellotti, F. Cariati, P. Fermo, M. Mellini, C. Viti, G. Padeletti, Heterogeneous distribution of metal nanocrystals in glazes of historical pottery, *Appl. Surf. Sci.* 185 (2002), 206-216.
54. J. Pérez-Arantegui, M. Resano, E. Garcia-Ruiz, F. Vanhaecke, C. Roldan, J. Ferrero, J. Coll, Characterization of cobalt pigments found in traditional Valencian ceramics by means of laser ablation-inductively coupled plasma mass spectrometry and portable X-ray fluorescence spectrometry, *Talanta* 74 (5) (2008), 1271-1280.
55. P. Colomban, F. Ambrosi, A. Ngo, T. Lu, X. Feng, S. Chen, C. Choi, Comparative analysis of Wucai Chinese porcelains using mobile and fixed Raman microspectrometers, *Ceram. Int.* 43 (2017), 14244-14256.
56. R. G. V. Hancock, J. McKechnie, S. Aufreiter, K. Karklins, M. Kapches, M. Sempowski, J. F. Moreau, I. Kenyon, Non-destructive analysis of European cobalt blue glass trade beads, *J. Radioanal. Nucl. Chem.* 244 (3) (2000), 567-573.
57. R. Montanari, M. F. Alberghina, A. Casanova Municchia, E. Massa, A. Pelagotti, C., Pelosi, S. Schiavone, A. Sodo, A polychrome Mukozuke (1624-1644) porcelain offers a new hypothesis on the introduction of European enamelling technology in Japan, *J. Cult. Herit.* 32 (2018), 232-237.
58. C. Fischer, E. Hsieh, Export Chinese blue-and-white porcelain: compositional analysis and sourcing using non-invasive portable XRF and reflectance spectroscopy, *J. Archaeol. Sci.* 80 (2017) 14-26.
59. F. Du, B. Su, Further study of sources of the imported cobalt-blue pigment used on Jingdezhen porcelain from late 13 to early 15 centuries, *Sci China Ser E-Tech Sci.* 51 (3) (2008) 249-259.

60. M. O. Figueiredo, T. P. Silva, J. P. Veiga, A XANES study of cobalt speciation state in blue-and-white glazes from 16th to 17th century Chinese porcelains, *J. Electron Spectrosc.* 185 (2012) 97-102.
61. R. Wen, A. M. Pollard, The pigments applied to Islamic Minai wares and the correlation with Chinese blue-and-white porcelain, *Archaeometry* 58 (1) (2016) 1-16.
62. T. Q. Zhu, Y. C. Zhang, H. Xiong, Z. Y. Feng, Q. Li, B.L. Cao, Comparison of the different types of Qinghua porcelain from Jingdezhen in the Yuan Dynasty of China (AD 1271-1368) by micro X-ray fluorescence spectroscopy ( $\mu$ -XRF) and microscopy, *Archaeometry* 58 (6) (2016) 966-978.
63. G. Pappalardo, E. Costa, C. Marchetta, L. Pappalardo, F. P. Romano, A. Zucchiatti, P. Prati, P. A. Mando, A. Migliori, L. Palombo, M.G. Vaccari, Non-destructive characterization of Della Robbia sculptures at the Bargello museum in Florence by the combined use of PIXE and XRF portable systems, *J. Cult. Herit.* 5 (2004) 183-188.
64. A. Zucchiatti, A. Bouquillon, I. Katona, A. D'Alessandro, The 'Della Robbia Blue': A case study for the use of cobalt pigments in ceramics during the Italian Renaissance, *Archaeometry* 48 (1) (2006) 131-152.
65. D. Barilaro, V. Crupi, S. Interdonato, D. Majolino, V. Venuti, G. Barone, M.F. La Russa, F. Bardelli, Characterization of blue decorated Renaissance pottery fragments from Caltagirone (Sicily, Italy), *Appl. Phys. A* 92 (2008) 91-96.
66. P. Munier, *Technologie des faïences*, Gauthier-Villars, Paris (France), 1957.

## Figure captions

Fig. 1: On-site studied shards excavated from the Iznik Tile Kilns (Turkey); see Table S2 for details. They were attributed to the productions from 14th- to 16th-centuries. The number 1 represents the shards having clayey body, and 3, calcareous body. The rest belongs to the group 2 which represents stonepaste tiles.

Fig. 2: On-site studied shards excavated from the Iznik Tile Kilns (Turkey) which were attributed to the 17th century production and the waste material (F1); see Table S2 and Fig.1 for details.

Fig.3: Scatter plots of the weight % ratios of  $\text{Al}_2\text{O}_3$  versus  $\text{SiO}_2$  (upper) and  $\text{K}/\text{Si}$  versus  $\text{Ca}/\text{Si}$  (bottom) in the body. Tiles of this study are grouped in five periods of production: 14-15th-c. (orange circle), 16th-c. (green circle), second half of 16th-c. (blue circle), 16-17th-c. (grey circle), 17th-c. (red circle) and one formation material of the kiln dated to unknown century (brown circle). Previous studies carried out with SEM-EDS were plotted in red open circles [28] & cross [2] (for redware type) and green open circles [28] & cross [2] (for stonepaste). Lines and circles are guide for eyes.

Fig. 4: Scatter plots of the weight % ratios of  $\text{K}/\text{Si}$  versus  $\text{Pb}/\text{Si}$  in the body (upper) and  $\text{Pb}$  versus  $\text{Si}$  (bottom) in the body, see previous figures for symbols.

Fig. 5: Scatter plots of the weight % ratios of  $\text{Sn}/\text{Si}$  versus  $\text{Pb}/\text{Si}$  (upper) and  $\text{Pb}/\text{Si}$  versus  $\text{Mg}/\text{Si}$  (bottom) in the transparent glaze, see previous figures for symbols. Lines are guide for eyes.

Fig. 6: Scatter plots of the weight % ratios of  $\text{Bi}/\text{Si}$  versus  $\text{Pb}/\text{Si}$  (upper) and  $\text{K}/\text{Si}$  versus  $\text{Ca}/\text{Si}$  (bottom) in the transparent glaze, see previous figures for symbols. Lines are guide for eyes.

Fig. 7: Scatter plots of the weight % ratios of  $\text{Co}/\text{Si}$  versus  $\text{As}/\text{Si}$  (upper left),  $\text{Co}/\text{Si}$  versus  $\text{Ni}/\text{Si}$  (upper right),  $\text{Mn}/\text{Si}$  versus  $\text{Co}/\text{Si}$  (bottom left) and  $\text{Bi}/\text{Si}$  versus  $\text{Co}/\text{Si}$  (bottom right) measured on blue areas; see previous figures for symbols. Lines are guide for eyes.

Fig. 8: Scatter plots of the weight % ratios of  $\text{Fe}/\text{Si}$  versus  $\text{Cu}/\text{Si}$  measured on red (upper left) and turquoise areas (upper right);  $\text{Cu}/\text{Si}$  versus  $\text{Fe}/\text{Si}$  (bottom left) and  $\text{Cu}/\text{Si}$  versus  $\text{Cr}/\text{Si}$  (bottom right) on green areas; see previous figures for symbols. Lines are guide for eyes.

Fig. 9: Evolution of the  $\text{Sn}/\text{Pb}$  (reference data obtained from 11,14,25,27)

Fig. 10: *left* Evolution of the  $\text{Co}/\text{Mn}$  ratio (reference data obtained from 47-64), *right* Ternary diagram of  $\text{Co}/\text{Si}$ ,  $\text{Mn}/\text{Si}$ , and  $\text{Ni}/\text{Si}$  showing the distribution of blue pigments of this study (solid circles) and reference data from the tiles of Edirne (open labels) [25].

## Highlights

- 1- First on-site, non-invasive pXRF analyses of tiles excavated at Iznik tile kilns
- 2- A new type of paste is evidenced for Iznik tiles which is rich in calcium.
- 3- Both European and Chinese cobalt sources were determined in the blue decors.



**Fig.1:** On-site studied shards excavated from the Iznik Tile Kilns (Turkey) which were attributed to the productions from 14th- to 17th-centuries; see Table S1 for details. The number 1 represents the shards having clayey body, and 3, calcareous body. The rest belongs to the group 2 which represents stonepaste tiles.

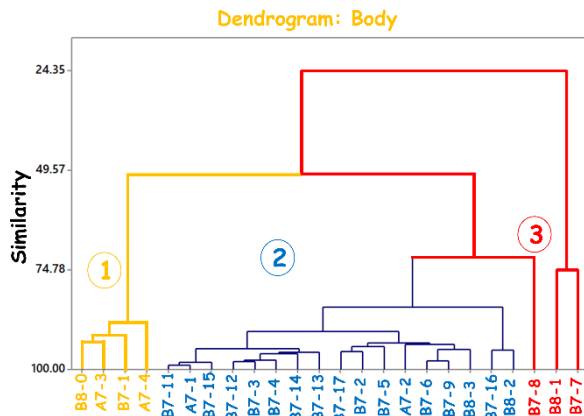
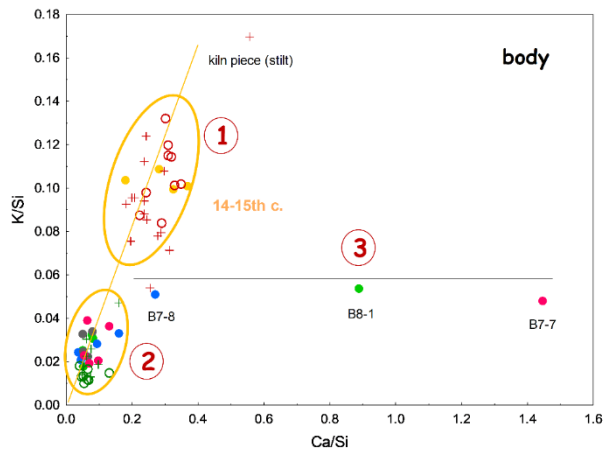
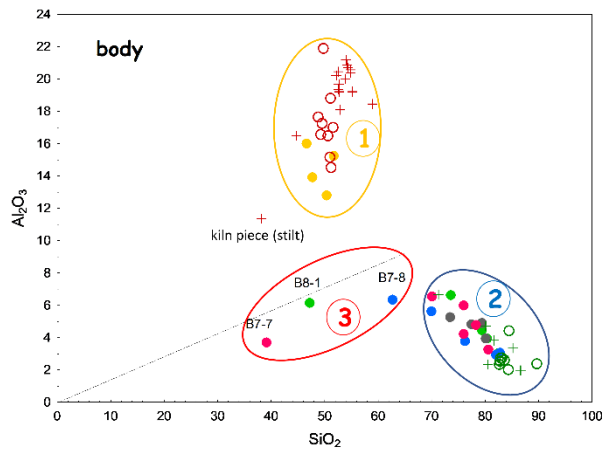


**Fig. 2:** Scatter plots of the weight % ratios of  $\text{Al}_2\text{O}_3$  versus  $\text{SiO}_2$  (upper) and  $\text{K/Si}$  versus  $\text{Ca/Si}$  (middle) in the body showing the tiles of five periods of production: 14-15th-c. (orange circle), 16th-c. (green circle), second half of 16th-c. (blue circle), 16-17th-c. (grey circle), 17th-c. (red circle) and one formation material of the kiln dated to unknown century (brown circle). Previous studies carried out with SEM-EDS were plotted in red open circles [28] & cross [2] (for redware) and green open circles [28] & cross [2] (for stonepaste). Lines and circles are guide for eyes. A dendrogram of the similarity on the body compositions (bottom) is plotted for better interpretation of the results by archaeologists.

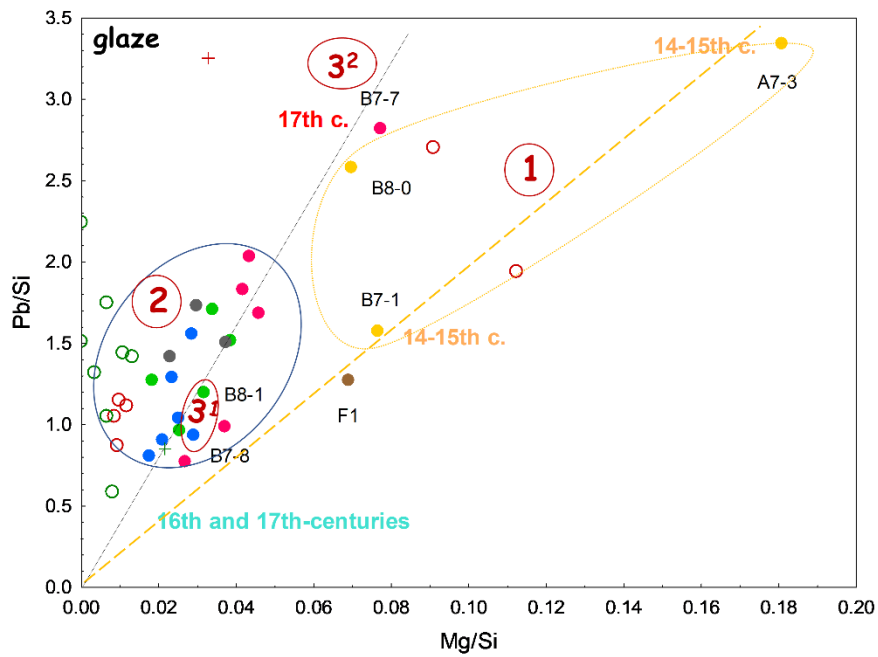
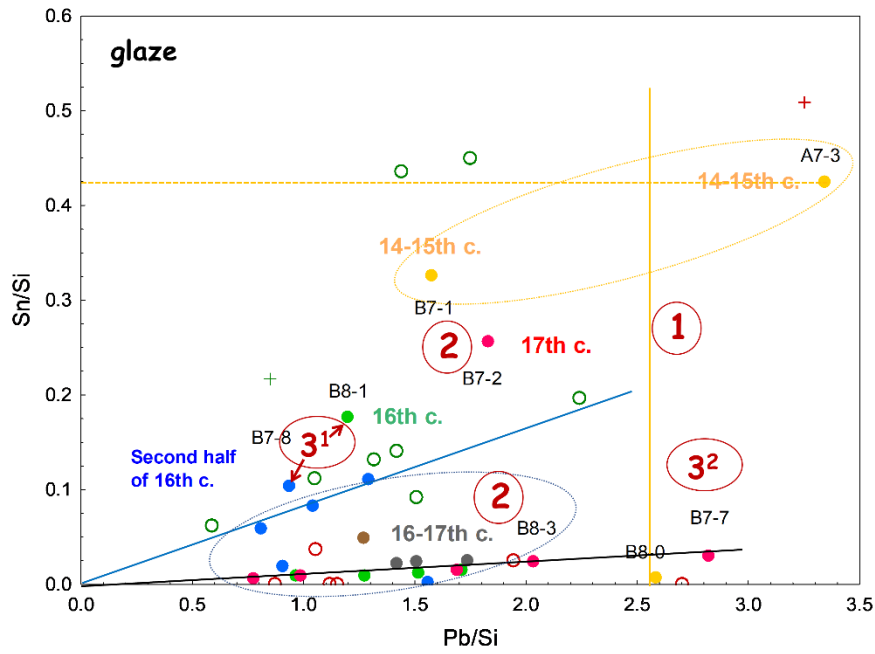


**Fig. 3:** Scatter plots of the weight % ratios of Sn/Si versus Pb/Si (upper) and Pb/Si versus Mg/Si (bottom) in the transparent glaze, see previous figures for symbols. Lines are guide for eyes.

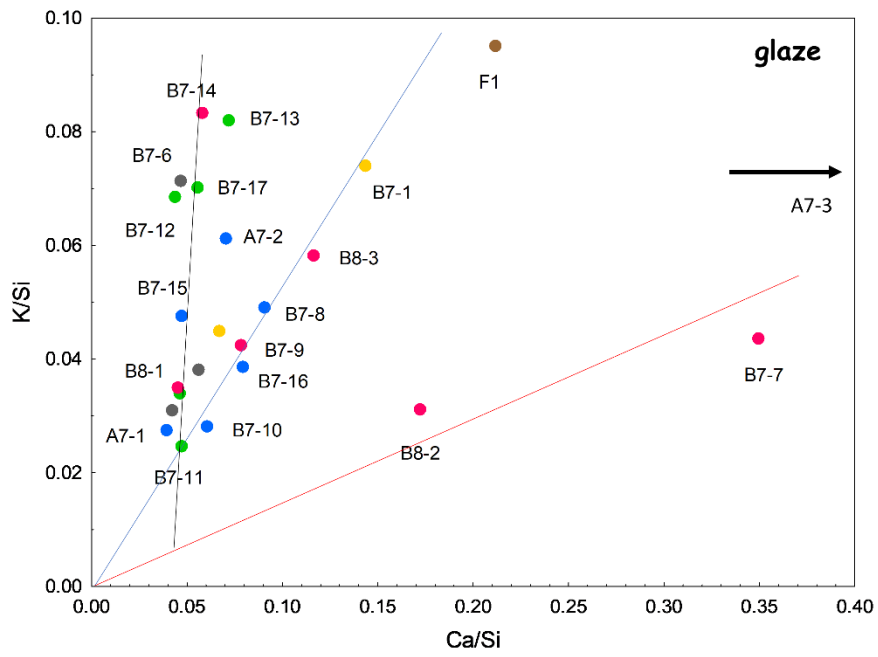
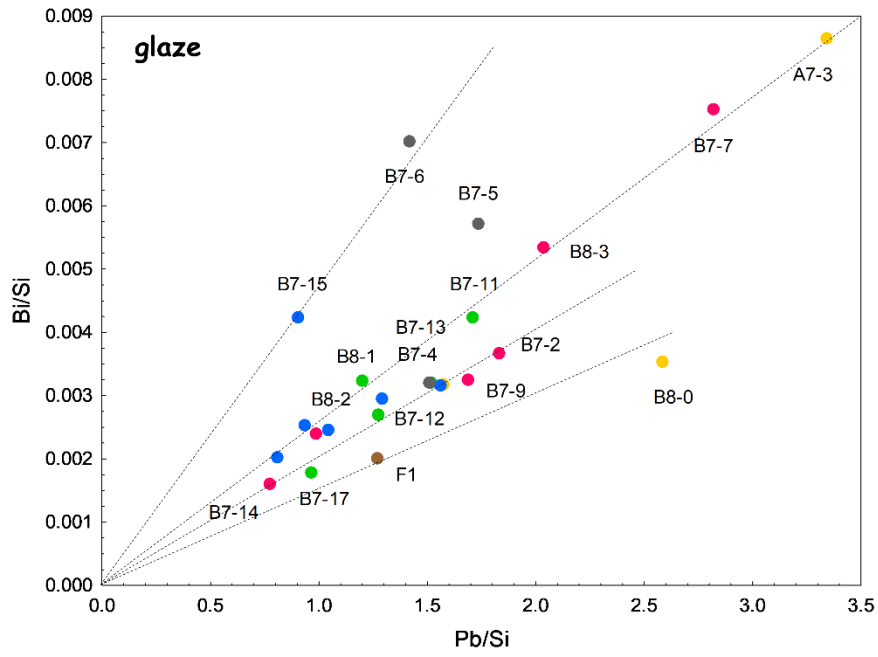


**Fig. 4:** Scatter plots of the weight % ratios of Bi/Si versus Pb/Si (upper) and K/Si versus Ca/Si (bottom) in the transparent glaze, see previous figures for symbols. Lines are guide for eyes.

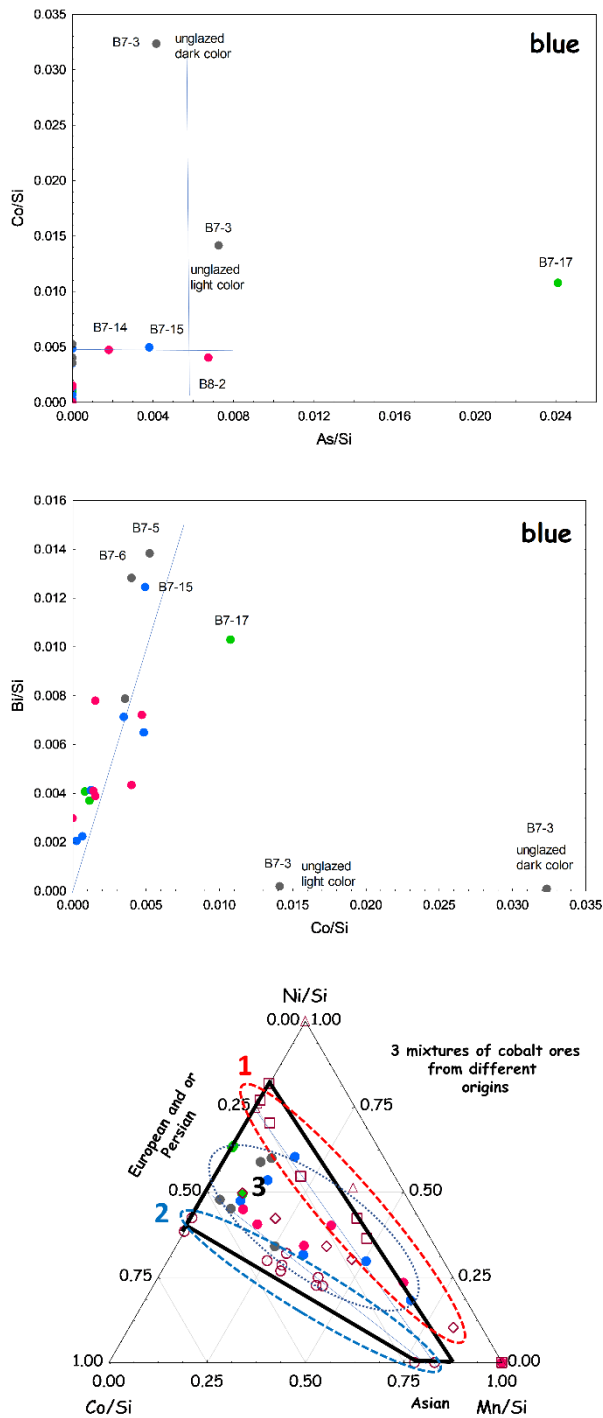


**Fig. 5:** Scatter plots of the weight % ratios of Co/Si versus As/Si (upper), Bi/Si versus Co/Si (middle) measured on blue areas, and ternary diagram (bottom) of Co/Si, Mn/Si, and Ni/Si showing the distribution of blue pigments of this study (solid circles) and reference data from the tiles of Edirne (open labels) [25]; see previous figures for symbols. Lines are guide for eyes.

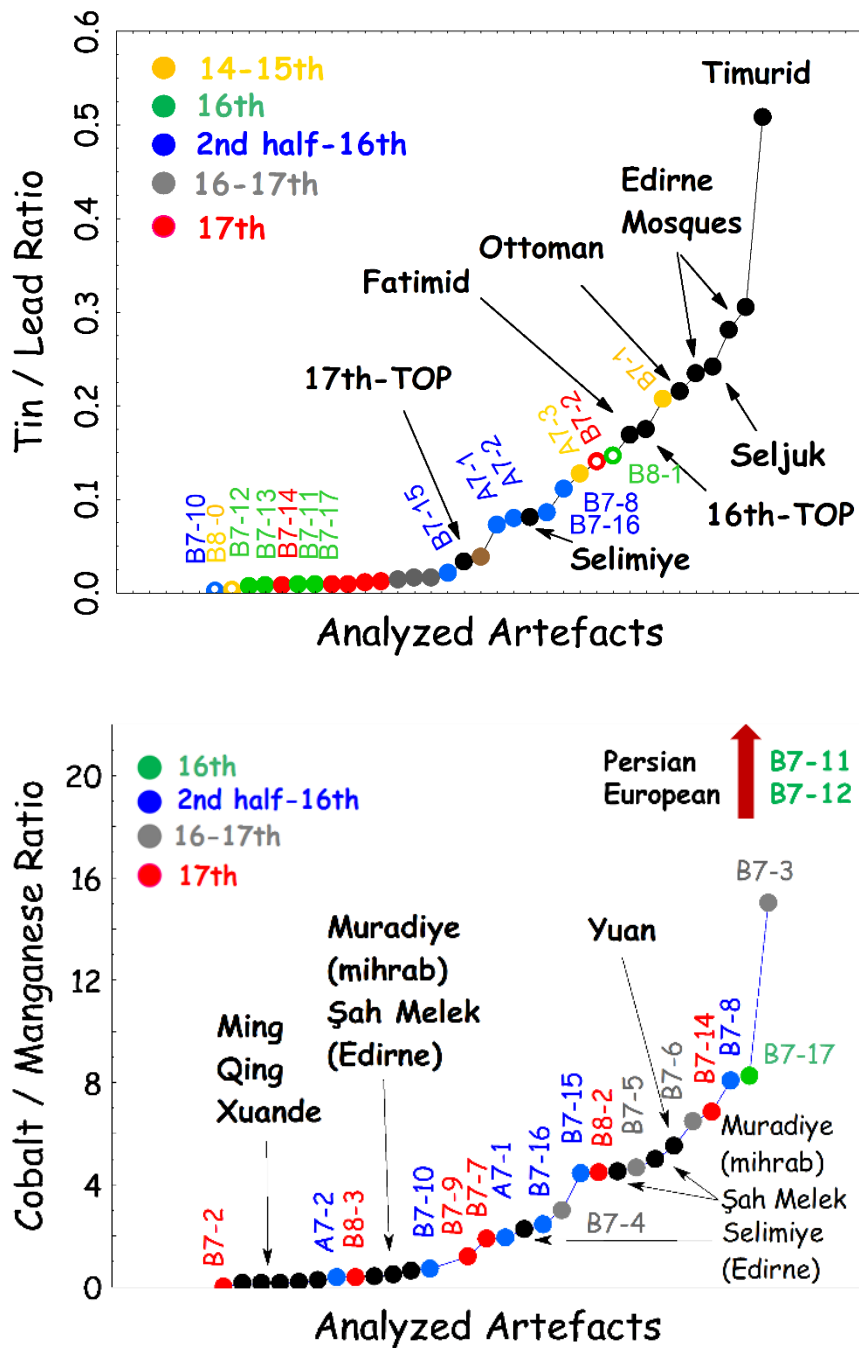


Fig. 6: upper Evolution of the Sn/Pb (reference data obtained from 11,14,25,27) and bottom Co/Mn ratio [47-64].

## **Supplementary Materials**

### **On-site pXRF analysis of glaze, body composition and colouring agents of tiles at the Iznik Tile Kilns Excavation**

Gulsu Simsek<sup>1</sup>, Belgin Demirsar Arlı<sup>2</sup>, Sennur Kaya<sup>3</sup>, Philippe Colombar<sup>4</sup>

<sup>1</sup> Koç University Surface Science and Technology Center (KUYTAM), Rumelifeneri Yolu, Sariyer 34450 Istanbul, Turkey

<sup>2</sup> Istanbul University, Faculty of Letters, Department of Art History, Balabanaga Mah., Laleli, Fatih, Istanbul

<sup>3</sup> Istanbul University, Department of Fine Arts, Balabanaga Mah. Laleli, Fatih, Istanbul

<sup>4</sup> Sorbonne Université, CNRS, MONARIS, Campus Pierre-et-Marie Curie, 75005, Paris, France

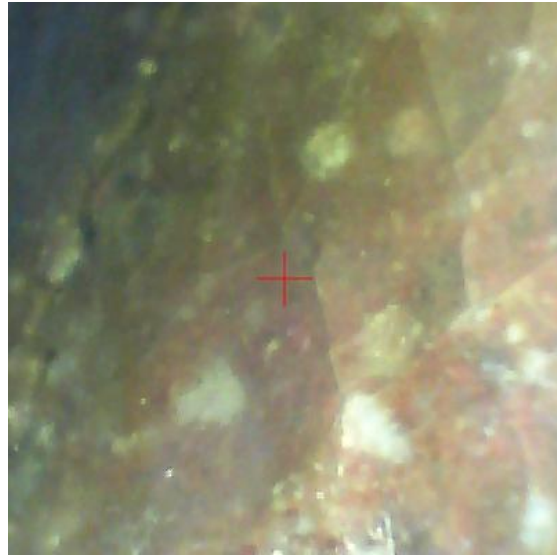


**Fig. S1:** View from the material which was formed on the walls inside of the kiln (left) and view from the analysis spot recorded with pXRF instrument.

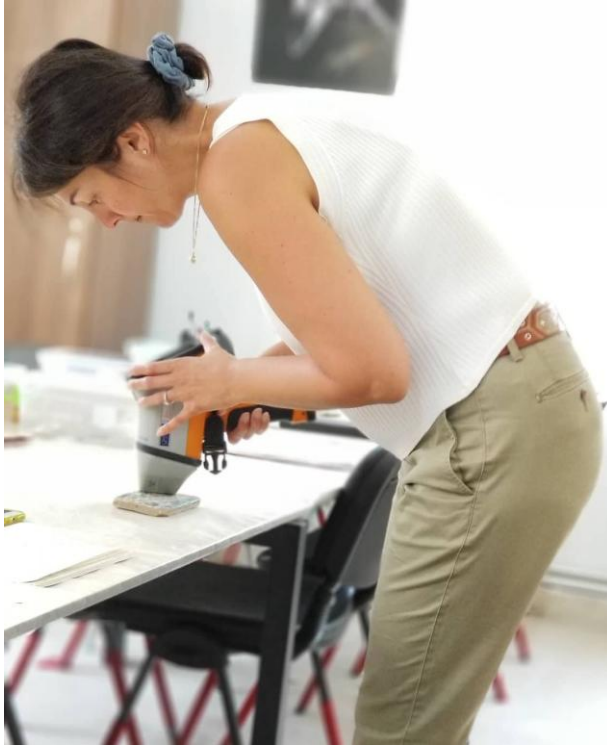


**Fig. S2:** On-site measurement in the excavation laboratory and Iznik Tile Kilns Excavation site.

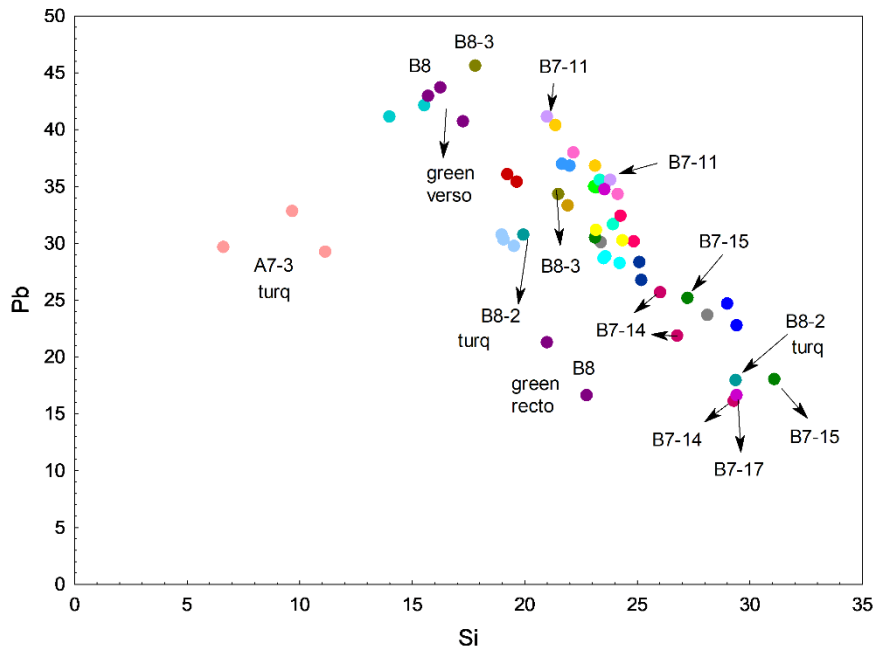


**Fig. S3** Scatter plots of the weight % of Pb versus Si showing all the measurements carried out in the transparent and colored glazes. Some of the tiles, especially the colored glazed shards, shows a larger variation. The variation in the transparent glazes originates from the change in the thickness of the glaze layer.

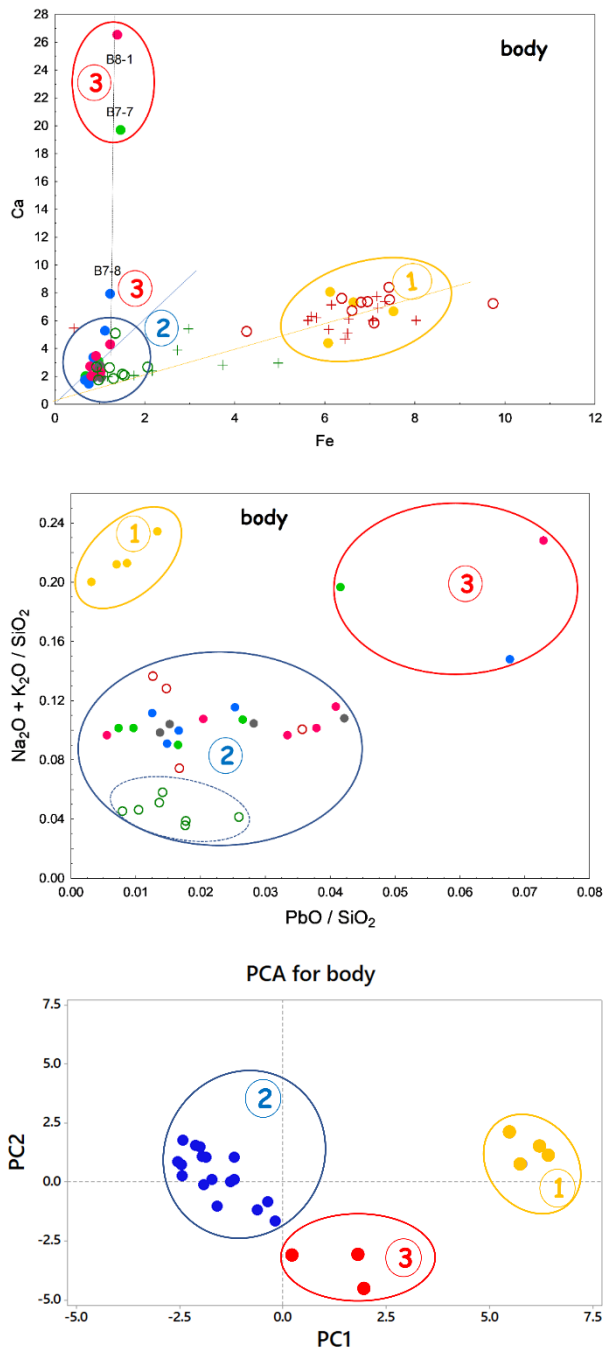


**Fig. S4:** Scatter plots of the weight % ratios of Ca versus Fe (upper) and  $\text{Na}_2\text{O} + \text{K}_2\text{O} / \text{SiO}_2$  versus  $\text{PbO} / \text{SiO}_2$  (bottom) found in the body showing the three groups of tiles compared with the reference shards including redware and fritware of Iznik kilns production [2, 28]; see text for symbols. Lines and circles are guide for eyes.

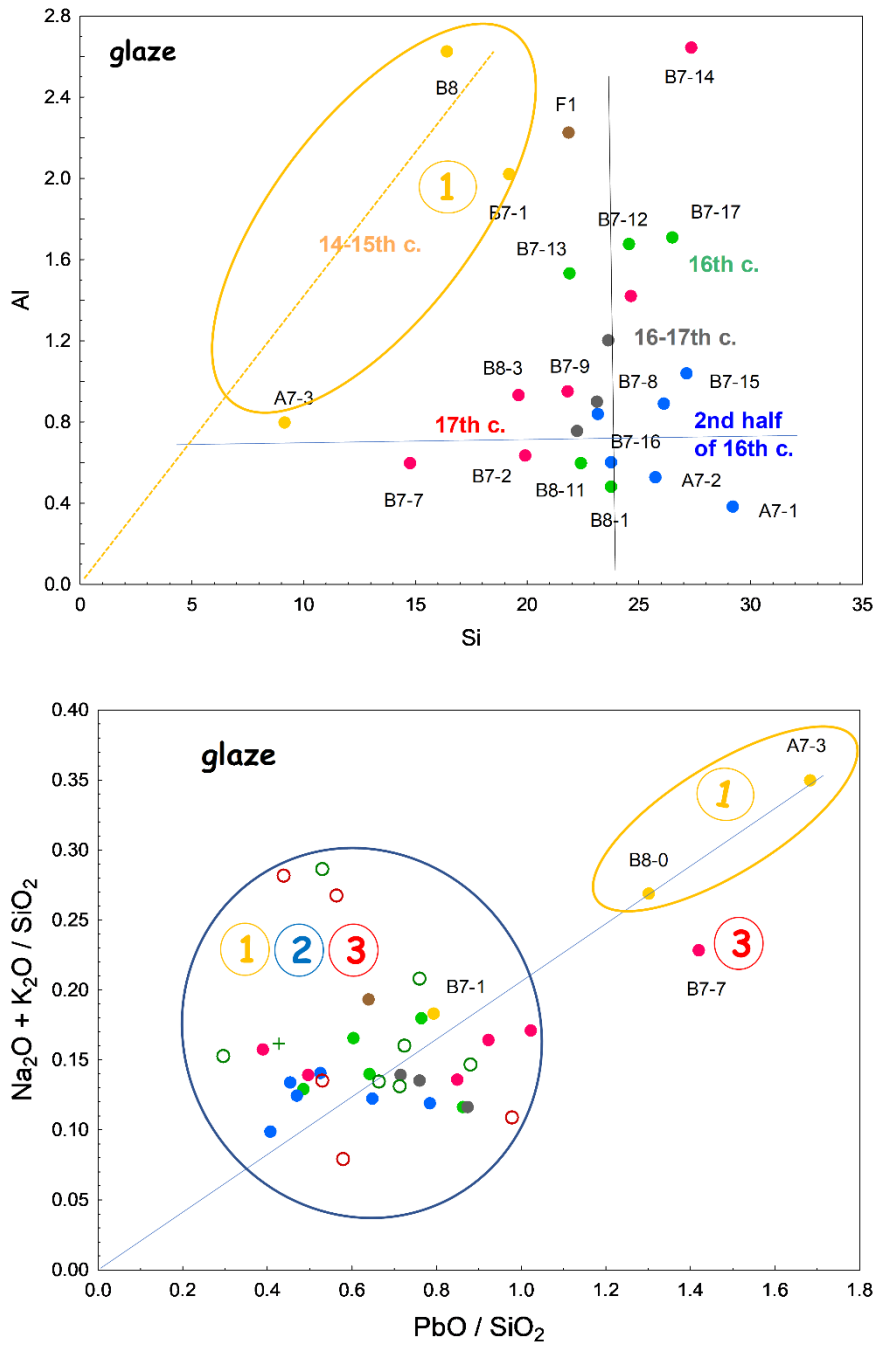


**Fig. S5:** Scatter plots of the weight % ratios of Al versus Si (upper) and  $\text{Na}_2\text{O} + \text{K}_2\text{O} / \text{SiO}_2$  versus  $\text{PbO} / \text{SiO}_2$  (bottom) found in the glaze; see text for symbols. Lines are guide for eyes.

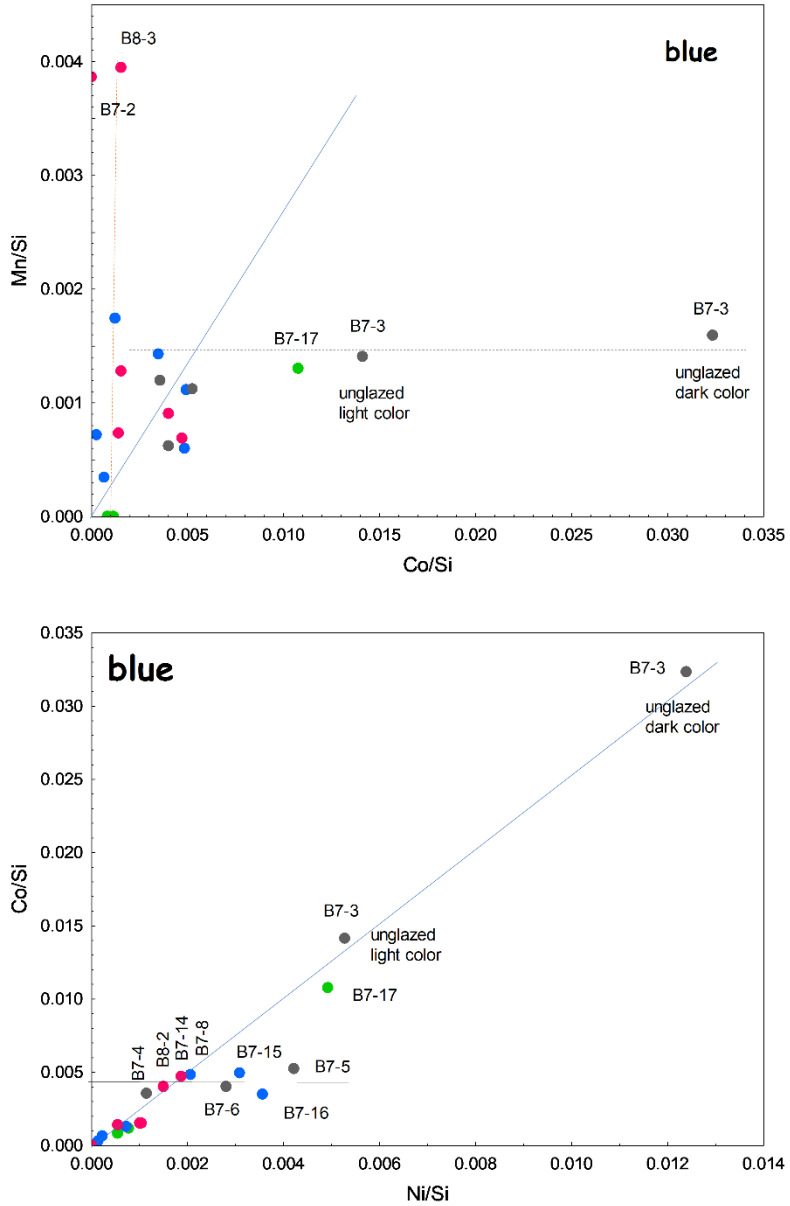


**Fig. S6:** Scatter plots of the weight % ratios of Mn/Si versus Co/Si (upper) and Co/Si versus Ni/Si (bottom) measured on blue areas; see text for symbols. Lines are guide for eyes.

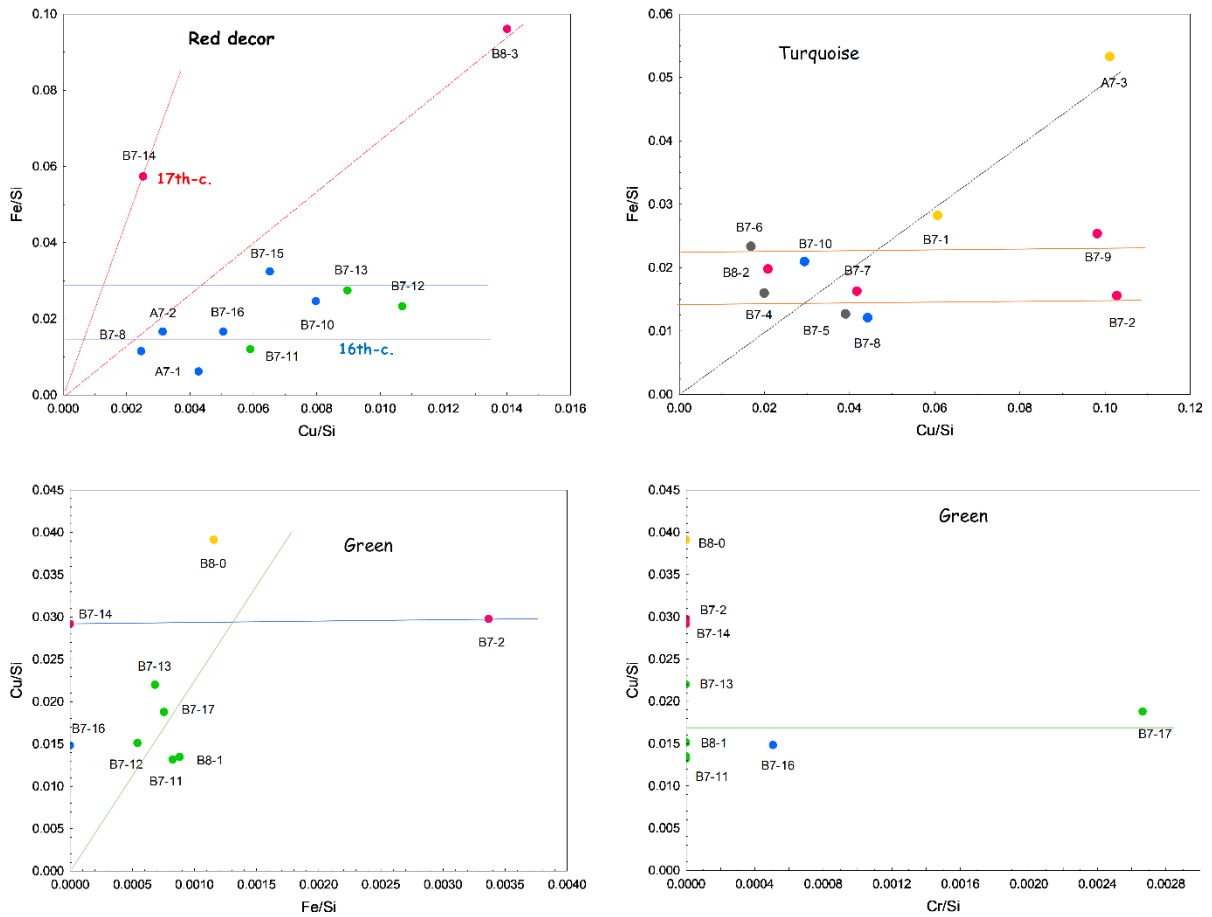


**Fig. S7:** Scatter plots of the weight % ratios of Fe/Si versus Cu/Si measured on red (upper left) and turquoise areas (upper right); Cu/Si versus Fe/Si (bottom left) and Cu/Si versus Cr/Si (bottom right) on green areas; see previous figures for symbols. Lines are guide for eyes.

**Table S1.** Description of the tiles showing the groups #1, #2, and #3 in accordance with their body composition

Production period	Code	Inventory number	Type	Group (Paste)	Type of decor	Areas measured with pXRF	
14-15th c.	B8-0	n.a.		#1	Glazed, Monochrome	Green (recto, verso), body	
	A7-3	IZN/18 BHD A7 ST4			Glazed, Monochrome	Turquoise, body	
	B7-1	IZN/18 BHD B7 ST2			Glazed, Monochrome	Turquoise, body	
	A7-4	IZN/18 BHD A7 ST1			Non-glazed, Biscuit	Body	
16th c.	B7-11	IZN/18 BHD B7 R24	Prototypes?	#2	Glazed, Polychrome	White, green, blue, red, body	
	B7-12	IZN/18 BHD B7 R24				White, red, green, blue, body	
	B7-13	n.a.				White, red, green, body	
	B7-17	IZN/18 BHD B7 Mb32	White, green, blue, body				
	B8-1	IZN/18 BHD B8 TR3			#3	Glazed, Monochrome	Green, body
Second half of 16th c.	B7-8	IZN/18 BHD B8 R4		#3	Glazed, Polychrome	Dark blue, turquoise, white, red, body, cross glaze	
	A7-1	IZN/18 BHD A7 R4	"classical"			#2	White, red, light and dark blue, contour, turquoise, body
	A7-2	IZN/18 BHD A7 R3					White, red, blue, contour, body
	B7-10	IZN/18 BHD B7 R2	Blue, white, turquoise, red				
	B7-15	IZN/18 BHD B7 R17	White, blue, orange, contour, body				
	B7-16	IZN/18 BHD B7 R1	White, blue, red, green, contour, body				
	16-17th c.	B7-3	IZN/18 BHD B7 Mb12				#3
B7-4		IZN/18 BHD B7 Mb33		Glazed, Polychrome	White, blue, turquoise, body		
B7-5		IZN/18 BHD B7 Mb30			White, blue, turquoise, body		
B7-6		IZN/18 BHD B7 Mb30			White, blue, turquoise, body		
17th c.	B8-2	IZN/18 BHD B7 Mb26		#3	Coloured glaze	Blue, turquoise, white, body	
	B8-3	IZN/18 BHD B8 R6				Green, white, red, contour, blue, body	
	B7-2	IZN/18 BHD B7 RS2			Glazed, Polychrome	Turquoise, green, contour, body	
	B7-9	IZN/18 BHD B7 Mb27				White, blue, turquoise, contour, body	
	B7-14	IZN/18 BHD B7 R29				White, green, blue, red, contour, body	
	B7-7	IZN/18 BHD B7 R3			Glazed, Polychrome (with Kaaba illustration)	Blue, white, turquoise, body	
Unknown	F-1	n.a.			Kiln material	Brown glassy layer	

**Table S2.** pXRF results of the body, glaze and decors (wt%)

<b>Code</b>	<b>Mg</b>	<b>Al</b>	<b>Si</b>	<b>P</b>	<b>K</b>	<b>Ca</b>	<b>Ti</b>	<b>Fe</b>	<b>Rb</b>	<b>Sr</b>	<b>Zr</b>	<b>Ba</b>	<b>Pb</b>	<b>Bi</b>	<b>S</b>
<b>B8</b>	2.509	8.467	21.799	0.463	2.200	8.029	0.809	6.115	0.015	0.031	0.023	0.055	0.578	0.000	0.000
<b>A7-3</b>	3.324	7.365	22.342	0.207	2.216	7.302	0.818	6.639	0.013	0.031	0.022	0.055	0.384	0.001	1.455
<b>A7-4</b>	3.460	8.054	24.187	0.172	2.500	4.378	0.773	6.073	0.012	0.020	0.018	0.048	0.151	0.000	1.050
<b>B7-1</b>	2.827	6.766	23.585	0.232	2.562	6.651	0.805	7.537	0.016	0.033	0.026	0.058	0.330	0.000	0.000
<b>B7-11</b>	0.997	1.600	38.531	0.159	0.680	2.005	0.000	0.683	0.004	0.010	0.004	0.023	1.270	0.003	0.000
<b>B7-12</b>	1.522	2.083	37.585	0.093	0.948	1.906	0.000	0.856	0.003	0.011	0.003	0.000	0.721	0.002	0.194
<b>B7-13</b>	0.931	2.349	37.132	0.135	1.135	3.090	0.000	0.974	0.003	0.011	0.003	0.026	0.546	0.001	0.000
<b>B7-17</b>	2.560	3.504	34.411	0.213	1.108	2.688	0.052	1.004	0.005	0.009	0.004	0.024	1.811	0.008	0.000
<b>B8-1</b>	2.356	3.253	22.109	0.689	1.181	19.671	0.127	1.472	0.007	0.031	0.010	0.052	1.828	0.007	0.050
<b>A7-1</b>	1.003	1.602	38.704	0.192	0.798	1.723	0.000	0.669	0.003	0.010	0.007	0.024	1.145	0.005	0.000
<b>A7-2</b>	1.756	1.988	35.669	0.545	0.999	3.339	0.077	0.859	0.003	0.012	0.007	0.025	0.887	0.005	0.360
<b>B7-8</b>	1.574	3.347	29.350	0.682	1.497	7.934	0.117	1.236	0.008	0.014	0.012	0.047	3.948	0.013	0.192
<b>B7-15</b>	1.155	1.557	38.391	0.100	0.927	1.466	0.000	0.768	0.004	0.009	0.005	0.026	1.273	0.011	0.147
<b>B7-16</b>	2.154	2.966	32.719	0.876	1.080	5.250	0.075	1.122	0.005	0.012	0.008	0.026	1.644	0.006	0.000
<b>B7-3</b>	1.234	2.070	37.465	0.121	1.217	1.917	0.000	1.040	0.005	0.012	0.004	0.023	1.135	0.004	0.000
<b>B7-4</b>	1.536	2.593	37.136	0.125	0.914	1.941	0.000	0.889	0.004	0.011	0.004	0.022	1.015	0.004	0.000

<b>B7-5</b>	1.801	2.783	34.378	0.320	1.163	2.765	0.706	1.000	0.007	0.014	0.006	0.056	2.879	0.015	0.000
<b>B7-6</b>	1.486	2.551	36.236	0.106	0.805	2.394	0.000	0.976	0.006	0.013	0.006	0.028	2.030	0.007	0.000
<b>B7-2</b>	1.988	3.157	35.567	0.116	1.378	2.282	0.048	1.023	0.005	0.011	0.004	0.024	1.447	0.003	0.000
<b>B7-7</b>	2.247	1.942	18.338	0.692	0.880	26.525	0.000	1.387	0.008	0.032	0.009	0.048	2.656	0.009	0.970
<b>B7-9</b>	1.441	2.518	36.612	0.189	0.827	1.999	0.000	0.814	0.005	0.012	0.005	0.029	2.433	0.006	0.000
<b>B7-14</b>	1.730	1.719	37.677	0.090	0.728	2.697	0.000	0.789	0.002	0.014	0.003	0.021	0.420	0.001	0.000
<b>B8-2</b>	2.202	3.456	32.804	0.342	1.184	4.299	0.098	1.240	0.007	0.015	0.007	0.036	2.663	0.007	0.000
<b>B8-3</b>	1.615	2.223	35.549	0.157	0.727	3.456	0.000	0.925	0.007	0.017	0.007	0.029	2.673	0.012	0.012

<b>Glaze</b>	<b>Mg</b>	<b>Al</b>	<b>Si</b>	<b>K</b>	<b>Ca</b>	<b>Fe</b>	<b>Sn</b>	<b>Pb</b>	<b>Bi</b>	<b>P</b>	<b>S</b>
<b>B8-0</b>	1.144	2.622	16.427	0.738	1.104	0.642	0.120	42.462	0.058	0.110	0.000
<b>A7-3</b>	1.652	0.794	9.144	0.615	20.781	0.487	3.880	30.579	0.079	0.210	1.228
<b>B7-1</b>	1.466	2.018	19.194	1.419	2.762	0.541	6.261	30.248	0.061	0.016	0.000
<b>B7-11</b>	0.761	0.597	22.405	0.550	1.061	0.247	0.333	38.374	0.095	0.202	0.000
<b>B7-12</b>	0.451	1.676	24.568	1.682	1.074	0.455	0.227	31.302	0.066	0.000	0.000
<b>B7-13</b>	0.841	1.529	21.911	1.794	1.581	0.546	0.254	33.284	0.070	0.000	1.251
<b>B7-17</b>	0.669	1.707	26.499	1.856	1.481	0.367	0.243	25.639	0.047	0.133	0.836
<b>B8-1</b>	0.756	0.478	23.786	0.808	1.109	0.320	4.208	28.571	0.077	0.170	0.000
<b>A7-1</b>	0.510	0.381	29.212	0.801	1.154	0.185	1.722	23.692	0.059	0.073	0.000

<b>A7-2</b>	0.647	0.525	25.752	1.573	1.815	0.461	2.142	26.887	0.063	0.092	0.000
<b>B7-8</b>	0.755	0.889	26.126	1.279	2.375	0.356	2.719	24.476	0.066	0.242	0.000
<b>B7-10</b>	0.658	0.837	23.158	0.652	1.403	0.346	0.057	36.144	0.073	0.174	0.000
<b>B7-15</b>	0.570	1.038	27.163	1.293	1.293	0.311	0.518	24.579	0.115	0.063	1.611
<b>B7-16</b>	0.558	0.601	23.758	0.915	1.892	0.240	2.631	30.669	0.070	0.654	0.000
<b>B7-4</b>	0.861	0.896	23.131	0.882	1.303	0.338	0.546	34.913	0.074	0.028	0.000
<b>B7-5</b>	0.661	0.753	22.247	0.688	0.948	0.210	0.558	38.621	0.127	0.139	0.000
<b>B7-6</b>	0.542	1.201	23.646	1.686	1.108	0.384	0.524	33.598	0.166	0.049	0.000
<b>B7-2</b>	0.830	0.634	19.920	0.695	0.903	0.463	5.113	36.501	0.073	0.030	0.000
<b>B7-7</b>	1.139	0.596	14.761	0.643	5.164	0.274	0.450	41.665	0.111	2.208	0.000
<b>B7-9</b>	1.000	0.949	21.833	0.924	1.712	0.365	0.337	36.878	0.071	0.184	0.000
<b>B7-14</b>	0.734	2.642	27.375	2.278	1.598	0.496	0.176	21.229	0.044	0.000	0.000
<b>B8-2</b>	0.915	1.418	24.661	0.765	4.252	0.535	0.221	24.337	0.059	0.948	0.349
<b>B8-3</b>	0.850	0.932	19.647	1.141	2.293	0.358	0.478	39.988	0.105	0.066	0.000
<b>F1</b>	1.512	2.225	21.864	2.067	2.649	1.837	1.074	27.833	0.053	0.000	0.000

<b>Blue area</b>	<b>Si</b>	<b>Mn</b>	<b>Fe</b>	<b>Co</b>	<b>Ni</b>	<b>Cu</b>	<b>Zn</b>	<b>As</b>	<b>Sn</b>	<b>Pb</b>	<b>Bi</b>
<b>B7-11</b>	28.307	0.000	0.257	0.033	0.022	0.123	0.007	0.000	0.354	39.747	0.105
<b>B7-12</b>	27.724	0.000	0.394	0.023	0.015	0.248	0.006	0.000	0.207	32.410	0.113

<b>B7-17</b>	20.720	0.027	0.600	0.223	0.102	0.174	0.008	0.500	0.281	36.438	0.213
<b>A7-1</b>	35.083	0.012	0.206	0.023	0.008	0.158	0.005	0.000	1.732	24.021	0.078
<b>A7-2</b>	36.396	0.026	0.443	0.010	0.005	0.088	0.016	0.000	1.858	23.256	0.075
<b>B7-8</b>	23.277	0.014	0.294	0.113	0.048	0.143	0.007	0.000	3.595	29.458	0.151
<b>B7-10</b>	20.686	0.036	0.384	0.026	0.015	0.093	0.016	0.000	0.084	41.059	0.085
<b>B7-15</b>	23.329	0.026	0.490	0.115	0.072	0.126	0.013	0.089	0.437	23.897	0.290
<b>B7-16</b>	14.016	0.020	0.237	0.049	0.050	0.155	0.009	0.000	2.559	30.177	0.100
<b>B7-3, dark decor</b>	25.166	0.040	1.638	0.814	0.312	0.019	0.004	0.105	0.000	0.826	0.002
<b>B7-3, light decor</b>	19.914	0.028	0.876	0.281	0.105	0.088	0.005	0.145	0.000	1.076	0.004
<b>B7-4</b>	20.104	0.024	0.374	0.072	0.023	0.301	0.010	0.000	0.518	34.147	0.158
<b>B7-5</b>	21.333	0.024	0.252	0.112	0.090	0.133	0.010	0.000	0.563	40.773	0.295
<b>B7-6</b>	24.200	0.015	0.425	0.097	0.068	0.200	0.008	0.000	0.498	33.322	0.310
<b>B7-2, thick border</b>	25.588	0.099	0.504	0.000	0.000	0.825	0.016	0.000	2.903	37.415	0.076
<b>B7-7</b>	27.163	0.020	0.274	0.038	0.015	0.099	0.014	0.000	0.450	41.665	0.111
<b>B7-9</b>	24.953	0.032	0.340	0.038	0.025	0.123	0.011	0.000	0.337	36.831	0.097
<b>B7-14</b>	20.287	0.014	0.651	0.096	0.038	0.116	0.008	0.037	0.186	24.657	0.146
<b>B8-2</b>	28.810	0.026	0.765	0.116	0.043	0.149	0.014	0.195	0.147	17.201	0.125
<b>B8-3</b>	18.224	0.072	0.413	0.028	0.019	0.318	0.017	0.000	0.565	39.326	0.142

<b>Red area</b>	<b>Si</b>	<b>Fe</b>	<b>Cu</b>	<b>Sn</b>	<b>Pb</b>
<b>B7-11</b>	21.004	0.253	0.124	0.355	40.263
<b>B7-12</b>	22.800	0.529	0.244	0.229	34.552
<b>B7-13</b>	22.820	0.627	0.205	0.236	32.824
<b>A7-1</b>	29.853	0.185	0.128	1.695	23.689
<b>A7-2</b>	28.673	0.478	0.090	1.671	22.676
<b>B7-8</b>	29.100	0.335	0.072	2.443	22.445
<b>B7-10</b>	17.061	0.421	0.136	0.092	37.802
<b>B7-15</b>	22.237	0.722	0.145	0.592	32.032
<b>B7-16</b>	24.367	0.405	0.123	2.543	30.316
<b>B7-14</b>	30.358	1.739	0.077	0.088	13.671
<b>B8-3</b>	20.634	1.983	0.289	0.363	32.120

<b>Black line</b>	<b>Mn</b>	<b>Fe</b>	<b>Cu</b>	<b>Cr</b>	<b>Co</b>	<b>Ni</b>
<b>A7-1</b>	0.016	0.206	0.143	0.000	0.000	0.000
<b>A7-2</b>	0.024	0.413	0.094	0.000	0.000	0.000
<b>B7-15</b>	0.026	0.709	0.735	0.598	0.000	0.018
<b>B7-16</b>	0.000	0.380	0.117	0.036	0.000	0.000
<b>B7-9</b>	0.015	0.325	0.099	0.055	0.020	0.012

<b>B7-14</b>	0.015	0.937	0.074	0.354	0.036	0.017
<b>B8-3</b>	0.035	0.605	0.287	0.157	0.020	0.012

<b>Turquoise area</b>	<b>Si</b>	<b>V</b>	<b>Mn</b>	<b>Fe</b>	<b>Cu</b>	<b>Cr</b>	<b>Co</b>	<b>Ni</b>	<b>Sn</b>	<b>Ba</b>
<b>A7-3</b>	9.144	0.239	0.100	0.487	0.925	0.000	0.000	0.000	3.880	0.066
<b>B7-1</b>	19.194	0.000	0.043	0.541	1.167	0.034	0.000	0.000	6.261	0.089
<b>B7-8</b>	24.715	0.219	0.016	0.297	1.094	0.046	0.032	0.013	3.843	0.082
<b>B7-10</b>	20.481	0.273	0.034	0.429	0.603	0.078	0.000	0.000	0.086	0.028
<b>B7-4</b>	23.360	0.253	0.032	0.372	0.467	0.033	0.082	0.018	0.534	0.066
<b>B7-5</b>	20.347	0.305	0.020	0.258	0.795	0.032	0.062	0.046	0.565	0.053
<b>B7-6</b>	21.666	0.221	0.000	0.505	0.365	0.035	0.128	0.092	0.579	0.076
<b>B7-2</b>	19.453	0.253	0.055	0.303	2.000	0.039	0.000	0.000	6.790	0.056
<b>B7-7</b>	15.379	0.336	0.000	0.250	0.643	0.046	0.000	0.000	0.458	0.119
<b>B7-9</b>	15.506	0.305	0.024	0.393	1.523	0.069	0.000	0.000	0.370	0.071
<b>B8-2</b>	28.678	0.000	0.023	0.567	0.597	0.038	0.019	0.009	0.153	0.027

<b>Green area</b>	<b>Si</b>	<b>V</b>	<b>Cr</b>	<b>Mn</b>	<b>Fe</b>	<b>Co</b>	<b>Ni</b>	<b>Cu</b>	<b>Sn</b>	<b>Ba</b>	<b>Pb</b>
<b>B8-0</b>	16.427	0.355	0.030	0.019	0.642	0.000	0.000	2.701	0.120	0.155	42.462
<b>B7-11</b>	20.552	0.290	0.034	0.017	0.270	0.000	0.000	1.306	0.371	0.000	38.013

<b>B7-12</b>	23.994	0.207	0.035	0.013	0.363	0.000	0.000	1.239	0.260	0.074	31.756
<b>B7-13</b>	23.399	0.000	0.046	0.016	0.514	0.000	0.000	1.007	0.250	0.048	31.291
<b>B7-17</b>	22.522	0.286	0.108	0.017	0.423	0.060	0.028	1.393	0.282	0.048	34.329
<b>B8-1</b>	23.786	0.210	0.216	0.021	0.320	0.000	0.006	2.058	4.208	0.042	28.571
<b>B7-16</b>	23.632	0.220	0.339	0.000	0.350	0.012	0.013	0.727	2.461	0.076	29.565
<b>B7-2</b>	19.593	0.290	0.464	0.066	0.583	0.000	0.007	0.978	5.657	0.061	36.353
<b>B7-14</b>	25.864	0.000	0.246	0.000	0.754	0.000	0.000	0.420	0.199	0.088	24.125

1

2 **Table S3.** Ratio of Sn versus Pb comparing the tiles of the study with the literature  
 3 [11,14,25,27]

<b>Tiles studied</b>	<b>Body Groups</b>	<b>Sn/Pb</b>	<b>Literature study</b>	<b>Sn/Pb</b>
B7-10	2	0.002	17th-century production (ref)	0.033
B8-0	1	0.003	Selimiye (Edirne)	0.081
B7-12	2	0.007	Fatimid	0.169
B7-13	2	0.008	16th-century production (ref)	0.175
B7-14	2	0.008	Ottoman	0.215
B7-11	2	0.009	Muradiye & Şah Melek Paşa (Edirne)	0.234
B7-17	2	0.009	Seljuk	0.242
B7-9	2	0.009	Yeşilce (Edirne)	0.281
B8-2	2	0.009	Şah Melek Paşa (Edirne)	0.305
B7-7	3	0.011	Timurid	0.508
B8-3	2	0.012		
B7-5	2	0.014		
B7-4	2	0.016		
B7-6	2	0.016		
B7-15	2	0.021		
F1	-	0.039		
A7-1	2	0.073		
A7-2	2	0.08		
B7-16	2	0.086		
B7-8	3	0.111		
A7-3	1	0.127		
B7-2	2	0.14		
B8-1	3	0.147		
B7-1	1	0.207		

4

1

2 **Table S4.** Ratio of Co versus Mn comparing the tiles of the study with the literature [25, 47-64].

<b>Tiles studied</b>	<b>Body Groups</b>	<b>Co/Mn</b>	<b>Literature study</b>	<b>Co/Mn</b>
B7-2	2	0	Chinese source: Ming	0.136
A7-2	2	0.385	Chinese source: Asbolite	0.138
B8-3	2	0.389	Chinese source: Qing	0.152
B7-10	2	0.722	Chinese source: Xuande	0.195
B7-9	2	1.188	Chinese source: Late Ming	0.245
B7-7	2	1.900	Selimiye – restoration (Edirne)	0.4
A7-1	2	1.917	Şah Melek Paşa – panel 1 (Edirne)	0.5
B7-16	2	2.450	Muradiye – mihrab (Edirne)	0.65
B7-4	2	3.000	Selimiye (Edirne)	2.25
B7-15	2	4.423	Şah Melek Paş – panel 2 (Edirne)	4.5
B8-2	2	4.462	Muradiye – mihrab (Edirne)	5
B7-5	2	4.667	Chinese source: Yuan	5.5
B7-6	2	6.467	Persian source	infinite
B7-14	2	6.857	European source	infinite
B7-8	3	8.071		
B7-17	2	8.259		
B7-3	2	15		
B7-11	2	Infinite		
B7-12	2	infinite		

3

4

5

6

7